FINITE ELEMENT SIMULATION OF NATURAL CONVECTION FROM AN OPEN RECTANGULAR CAVITY CONTAINING ADIABATIC CIRCULAR CYLINDER
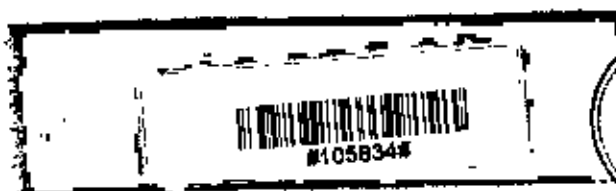
BY

FARIZA TUL KOABRA
Student No. 040509010P
Registration No. 0405410, Session: April-2005

MASTER OF PHILOSOPHY
IN
MATHEMATICS

DEPARTMENT OF MATHEMATICS
BANGLADESH UNIVERSITY OF ENGINEERING AND TECHNOLOGY
DHAKA-1000
SEPTEMBER-2008

The thesis titled
FINITE ELEMENT SIMULATION OF NATURAL CONVECTION FROM AN OPEN
RECTANGULAR CAVITY CONTAINING ADIABATIC CIRCULAR CYLINDER

Submitted by
FARIZA TUL KOABRA
Student No. 040509010P, Registration No. 0405410, Session: April-2005, a part time student of
M. Phil. (Mathematics) has been accepted as satisfactory in partial fulfillment for the degree of
Master of Philosophy in Mathematics
On 23, September- 2008

BOARD OF EXAMINERS

1. A. Alim
    23/9/08
    Dr. Md. Abdul Alim   Chairman
    Assistant Professor   (Supervisor)
    Department of Mathematics
    BUET, Dhaka-1000

2. Dr. Md. Abdul Maleque   Member
    Professor and Head   (Ex-Officio)
    Department of Mathematics
    BUET, Dhaka-1000

3. Dr. Md. Mustafa Kamal Chowdhury   Member
    Professor
    Department of Mathematics,
    BUET, Dhaka-1000

4. 23. 9. 08
    Md. Obayedullah   Member
    Associate Professor
    Department of Mathematics.
    BUET, Dhaka-1000

5. 23.09.08
    Dr. Amal Krishna Halder   Member
    Professor   (External)
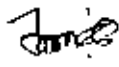   Department of Mathematics,
    Dhaka University, Dhaka-1000

ABSTRACT

A numerical simulation of two-dimensional laminar steady-state natural convection in a rectangular open cavity has been investigated. An adiabatic circular cylinder is placed at the center of the cavity and the opposite wall to the aperture is heated by a constant heat flux. The top and bottom walls are kept at the constant temperature. The fluid is concerned with Prandtl numbers 0.72, 1.0 and 7.0. The properties of the fluid were assumed to be constant. The physical problems are represented mathematically by different sets of governing equations along with the corresponding boundary conditions. In this thesis, a finite element method for steady-state incompressible natural convection flows has been developed. The non-dimensional governing equations are discretized by using Galerkin weighted residual method of finite element formulation. The obtained results are presented in terms of streamlines and isotherms, heat transfer characteristics Nusselt numbers for Grashof numbers from 10^3 to 10^6 and for an inclination angles of the cavity ranges for $0°, 15°, 30°$ and $45°$. The obtained results are also presented with the variation of different diameter ratios of the cylinder. The results show that the Nusselt numbers increase with the increasing of Grashof numbers. Also the Nusselt number changes substantially with the inclination angle of the cavity while better thermal performance is also sensitive to the boundary condition of the heated wall. Mesh refinement led to solutions for Grashof numbers from 10^3 to 10^6.

Author's Declaration

I am hereby declaring that the work in this dissertation was carried out in accordance with the regulations of Bangladesh University of Engineering and Technology (BUET), Dhaka, Bangladesh. The work is also original except where indicated by and attached with special reference in the context and no part of it has been submitted for any attempt to get other degrees or diplomas.

All views expressed in the dissertation are those of the author and in no way or by no means represent those of Bangladesh University of Engineering and Technology, Dhaka. This dissertation has not been submitted to any other University for examination either in home or abroad.

23.09.08

(FARIZA TUL KOABRA)

Date. 23 September, 2008

Acknowledgements

CONTENTS

Nomenclature

g	gravitational acceleration (ms^{-2})
Gr	Grashof number
k	thermal conductivity of the fluid $(Wm^{-1}K^{-1})$
L	height and width of the enclosure (m)
D	Diameter of the cylinder
Nu	Nusselt number
p	pressure (Nm^{-2})
P	non-dimensional pressure
Pr	Prandtl number, v/α
q	heat flux (Wm^{-2})
dr	Diameter ratio
T	temperature (K)
u, v	velocity components (ms^{-1})
U, V	non-dimensional velocity components
x, y	Cartesian coordinates (m)
X, Y	non-dimensional Cartesian coordinates

Greek symbols

α	thermal diffusivity, (m^2s^{-1})
β	thermal expansion coefficient (K^{-1})
ρ	density of the fluid (kgm^{-3})
v	kinematic viscosity of the fluid (m^2s^{-1})
θ	non-dimensional temperature
Φ	inclination angle of the cavity

List of Tables

List of Figures

INTRODUCTION

1.1 GENERAL

Heat transfer is that science which seeks to predict the energy transfer which may take place between material bodies as a result of a temperature difference. Thermodynamics teaches that this energy transfer is defined as heat. The science of heat transfer seeks not merely to explain how heat energy may be transferred, but also to predict the rate at which the exchange will take place under certain specified conditions.

The phenomenon of heat transfer was known to human being even in the primitive age when they used to use solar energy as a source of heat. Heat transfer in its initial stage was conceived with the invention of fire in the early age of human civilization. Since then its knowledge and use has been progressively increasing each day as it is directly related to the growth of human civilization. With the invention of stream engine by James watt in 1765 A. D., the phenomenon of heat transfer got its first industrial recognition and after that its use extended to a great extent and spread out in different spheres of engineering fields. In the past three decades, digital computers, numerical techniques and development of numerical models of heat transfer have made it possible to calculate heat transfer of considerable complexity and thereby create a new approach to the design of heat transfer equipment.

The study of the universe has led to the realization that all physical phenomena are subject to natural laws. The term natural might well be used to describe the framework or system of fundamental and universal importance within this system is the mechanisms for the transfer of heat. Heat transfer is a branch of applied thermodynamics. It estimates the rate at which heat is transferred across the system boundaries subjected to specific temperature differences and the temperature distribution of the system during the process. Whereas classical thermodynamics deals with the amount of heat transferred during the process. Heat transfer processes have always been an integral part of our environment.

The study of temperature and heat transfer is of great importance to the engineers because of its almost universal occurrence in many branches of science and engineering. Although heat transfer analysis is most important for the proper sizing of fuel elements in the nuclear reactors cores to prevent burnout, the performance of aircraft also depends upon the ease with which the structure and engines can be cooled. The design of chemical plants is usually done on the basis of heat transfer analysis and the analogous mass transfer processes. The transfer and conversion of

energy from one form to another is the basis to all heat transfer process and hence, they are governed by the first as well as the second law of thermodynamics. Heat transfer is commonly associated with fluid dynamics. The knowledge of temperature distribution is essential in heat transfer studies because of the fact that the heat flow takes place only wherever there is a temperature gradient in a system. The heat flux which is defined as the amount of heat transfer per unit area in per unit time can be calculated from the physical laws relating to the temperature gradient and the heat flux.

1.2 HEAT TRANSFER MECHANISM

Heat is the form of energy that can be transferred from one system to another as a result of temperature difference. A thermodynamic analysis is concerned with the amount of heat transfer as a system undergoes a process from one equilibrium state to another. The science that deals with the determination of the rates of such energy transfers is the heat transfer. The transfer of energy as heat is always from the higher temperature medium to the lower temperature one, and heat transfer stops when the two mediums reach the same temperature.

Heat can be transferred in three different mechanisms or modes: conduction, convection and radiation. All modes of heat transfer require the existence of a temperature difference, and all modes are from the high temperature medium to a lower temperature one. In reality, the combined effect of these three modes of heat transfer control temperature distribution in a medium. A brief description of convection mode is given below.

1.3 CONVECTION

Convective heat transfer is the heat transfer mechanism affected by the flow of fluids. The amount of energy and matter are conveyed by the fluid can be predicted through the convective heat transfer. The convective heat transfer bifurcates into two branches; the natural convection and the forced convection. Forced convection regards the heat transport by induced fluid motion that is forced to happen. This induced flow needs consistent mechanical power. But natural convection differs from the forced convection through the fluid flow driving force that happens naturally. The flows are driven by the buoyancy effect due to the presence of density gradient and gravitational field. The density difference gives rise to buoyancy effects due to which the flow is generated. Buoyancy is due to the combined presence of the fluid density gradient and the body force. As the temperature distribution in the natural convection depends on the intensity of the fluid currents that is dependent on the temperature potential itself, the qualitative and quantitative analysis of natural convection heat transfer is very difficult. Numerical investigation instead of theoretical analysis is more needed in this field. Two types of natural convection heat transfer phenomena can be observed in the nature. One is that external free convection that is

caused by the heat transfer interaction between a single wall and a very large fluid reservoir adjacent to the wall. Another is that internal free convection which befalls within an enclosure. The thermo-fluid fields developed inside the cavity depend on the orientation and geometry of the cavity. Reviewing the nature and the practical applications, the enclosure phenomena can be organized into two classes. One of these is enclosure heated from the side which is found in solar collectors, double wall insulations, laptop cooling system and air circulation inside the room and another one is enclosure heated from below which happens in geophysical system like natural circulation in the atmosphere, the hydrosphere and the molten core of the earth.

Convective heat transfer or, simply, convection is the study of heat transport processes affected by the flow of fluids. Convective heat transfer, clearly, is a field at the interface between two older fields-heat transfer and fluid mechanics. Before reviewing the foundations of convective heat transfer methodology, it is worth reexamining the historic relationship between fluid mechanics and heat transfer at the interface. Especially during the past 100 years, heat transfer and fluid mechanics have enjoyed a symbiotic relationship in their parallel development. Convection is that mode of heat transfer where energy exchange occurs between the particles by convection current. It may be explained as; when fluid flows over a solid body or inside a channel while temperatures of the fluid and the solid surface are different, heat transfer between the fluid and the solid surface takes place as a consequences of the motion of the fluid relative to the surfaces; the mechanism of heat transfer called convection. In the diversity of the studies related to heat transfer, considerable effort has been directed at the convective mode, in which the relative motion of the fluid provides an additional mechanism for the transfer of heat and materials. Convection is inevitably coupled with the conductive mechanism, since though the fluid motion modifies the transport process, the eventual transfer of heat from one fluid element to another in its neighborhood is through conduction.

The convection mode of heat transfer is further divided into two basic processes. If the motion of the fluid arises due to an external agent, such as the externally imposed flow of fluid stream over a heated object, the process is termed as forced convection. The fluid flow may be the results of, for instance, a fan, a blower, the wind or the motion of the heated object itself. Such problems are very frequently encountered in technology where heat transfer to, or from, a body is often due to an imposed flow of a fluid at a temperature different from that of the body. It has wide applications in compact heat exchanger, central air conditioning system, cooling tower, gas turbine blade, internal cooling passage, chemical engineering process industries, nuclear reactors and many other cases. If, on the other hand, no such externally induced flow is provided and the flow arises "naturally" simply due to the effect of a density difference, resulting from a temperature difference, in a body force field, such as gravitational field, the process is termed as natural or free convection. The density deference gives rise to buoyancy effects due to which the

3

flow is generated. A heated body cooling in ambient air generates such a flow in the region surrounding it. Similarly, the buoyant flow arising from heat rejection to the atmosphere and to other ambient media, Heat transfer by free convection occurs in many engineering applications, such as heat transfer from hot radiators, refrigerator coils, transmission lines, electric transformers, electric heating elements and electronic equipment etc.

The convection heat transfer that is neither dominated by pure forced nor pure free convection, but is rather a combination of the two is referred as combined or mixed convection. The buoyancy forces that arise as the results of the temperature differences and which cause the fluid flow in free convection also exist when there is a forced flow. The effects of these buoyancy forces are however; usually negligible when there is a forced flow. In some cases, however, these buoyancy forces do have a significant influence on the flow and consequently on the heat transfer rate. In such cases, the flow about the body is a combination of forced and free convection; such flows are referred to as mixed convection. For example, heat transfer from one fluid to another fluid through the walls of pipe occurs in many practical devices. In this case, heat is transferred by convection from the hotter fluid to the one surface of the pipe. Heat is then transferred by conduction through the walls of the pipe. Finally, heat is transferred by convection from the other surface to the colder fluid.

1.4 SOME DEFINITIONS

Some basic definitions that are related to the current study are presented below.

1.4.1 THERMAL CONDUCTIVITY

Thermal conductivity of a material can be defined as the rate of heat transfer through a unit thickness of the material per unit area per unit temperature difference. Therefore the thermal conductivity of a material is a measure of the ability of the material to conduct heat. A high value for thermal conductivity indicates that the material is a good heat conductor, and a low value for thermal conductivity indicates that the material is a poor heat conductor or insulator. For example the materials such as copper and silver that are good electric conductors are also good heat conductors, and have high values of thermal conductivity. Materials such as rubber, wood are poor conductors of heat and have low conductivity values. The rate of heat conduction through a medium depends on the geometry of the medium, its thickness, and the material of the medium, as well as the temperature difference across the medium. The proportionality constant k is called thermal conductivity of the material.

1.4.2 THERMAL DIFFUSIVITY

The time dependent heat conduction equation for constant k contains a quantity α, called the thermal diffusivity. Thermal diffusivity represents how fast heat diffuses through a material and is defined as

$$\alpha = \frac{\kappa}{\rho C_p}$$

Here the thermal conductivity κ represents how well a material conducts heat, and the heat capacity ρC_p represents how much energy a material stores per unit volume. Therefore, the thermal diffusivity of a material can be viewed as the ratio of the heat conducted through the material to the heat stored per unit volume. A material that has a high thermal conductivity or a low heat capacity will obviously have a large thermal diffusivity. The larger thermal diffusivity means that the propagation of heat into the medium is faster. A small value of thermal diffusivity means the material mostly absorbs the heat and a small amount of heat is conducted further.

1.4.3 INTERNAL AND EXTERNAL FLOWS

A fluid flow is classified as being internal or external, depending on whether the fluid is forced to flow in a confined channel or over a surface. An internal flow is bounded on all sides by solid surfaces except, possibly, for an inlet and exit. Flows through a pipe or in an air-conditioning duct are the examples of internal flow. Internal flows are dominated by the influence of viscosity throughout the flow field. The internal flow configuration represents a convenient geometry for the heating and cooling of fluids used in the chemical processing, environmental control, and energy conversion areas. The flow of an unbounded fluid over a surface is external flow. The flows over curved surfaces such as sphere, cylinder, airfoil, or turbine blade are the example of external flow. In external flows the viscous effects are limited to boundary layers near solid surfaces.

1.4.4 BOUNDARY LAYER

Since fluid motion is the distinguishing feature of heat convection, it is necessary to understand some of the principles of fluid dynamics in order to describe adequately the processes of convection. When a fluid flows over a body, the velocity and temperature distribution at the immediate vicinity of the surface strongly influence by the convective heat transfer. In order to simplify the analysis of convective heat transfer the boundary layer concept frequently is introduced to model the velocity and temperature fields near the solid surface in order to simplify the analysis of convective heat transfer. So we are concerned with two different kinds of boundary layers, the velocity boundary layer and the thermal boundary layer.

The velocity boundary layer is defined as the narrow region, near the solid surface, over which velocity gradients and shear stresses are large, but in the region outside the boundary layer, called the potential-flow region, the velocity gradients and shear stresses are negligible. The exact limit of the boundary layer cannot be precisely defined because of the asymptotic nature of the velocity variation. The limit of the boundary layer is usually taken to be at the distance from the surface, at which the fluid velocity is equal to a predetermined percentage of the free stream value, U_∞. This percentage depends on the accuracy desired, 99 or 95% being customary. Although, outside the boundary layer region the flow is assumed to be inviscid, but inside the boundary layer the viscous flow may be either laminar or turbulent. In the case of laminar boundary layer, fluid motion is highly ordered and it is possible to identify streamlines along which particles move. Fluid motion along a streamline is characterized by velocity components in both the x and y directions. Since the velocity component v is in the direction normal to the surface, it can contribute significantly to the transfer of momentum, energy or species through the boundary layer. Fluid motion normal to the surface is necessitated by boundary layer growth in the x direction. In contrast, fluid motion in the turbulent boundary layer is highly irregular and is characterized by velocity fluctuations. These fluctuations enhance the transfer of momentum, energy and species and hence increase surface friction, as well as convection transfer rates. Due to fluid mixing resulting from the fluctuations, turbulent boundary layer thicknesses are larger and boundary layer profiles are flatter than in laminar flow. The thermal boundary layer may be defined (in the same sense that the velocity boundary layer was defined above) as the narrow region between the surface and the point at which the fluid temperature has reached a certain percentage of ambient temperature T_∞. Outside the thermal boundary layer the fluid is assumed to be a heat sink at a uniform temperature of T_∞. The thermal boundary layer is generally not coincident with the velocity boundary layer, although it is certainly dependent on it. If the fluid has high thermal conductivity, it will be thicker than the velocity boundary layer, and if conductivity is low, it will be thinner than the velocity boundary layer.

1.4.5 FLOW WITHIN AN ENCLOSURE

The flow within an enclosure consisting of two horizontal walls, at different temperatures, is an important circumstance encountered quite frequently in practice. In all the applications having this kind of situation, heat transfer occurs due to the temperature difference across the fluid layer, one horizontal solid surface being at a temperature higher than the other. If the upper plate is the hot surface, then the lower surface has heavier fluid and by virtue of buoyancy the fluid would not come to the lower plate. Because in this case the heat transfer mode is restricted to only conduction. But if the fluid is enclosed between two horizontal surfaces of which the upper surface is at lower temperature, there will be the existence of cellular natural convective currents

which are called as Benard cells. For fluids whose density decreases with increasing temperature, this leads to an unstable situation.

1.4.6 TILTED ENCLOSURE

The tilted enclosure geometry has received considerable attention in the heat transfer literature because of mostly growing interest of solar collector technology. The angle of tilt has a dramatic impact on the flow housed by the enclosure. Consider an enclosure heated from below is rotated about a reference axis. When the tilted angle becomes 90°, the flow and thermal fields inside the enclosure experience the heating from side condition. Thereby convective currents may pronounce over the diffusive currents. When the enclosure rotates to 180°, the heat transfer mechanism switches to the diffusion because the top wall is heated.

1.4.7 BOUSSINESQ APPROXIMATION

The governing equations for convection flow are coupled elliptic partial differential equations and are, therefore, of considerable complexity. The major problems in obtaining a solution to these equations lie in the inevitable variation of density with temperature, or concentration, and in their partial, elliptic nature. Several approximations are generally made to considerably simplify these equations. Among them Boussinesq approximation attributed to Boussinesq (1903) is considered here. In flows accompanied by heat transfer, the fluid properties are normally functions of temperature. The variations may be small and yet be the cause of the fluid motion. If the density variation is not large, one may treat the density as constant in the unsteady and convection terms, and treat it as variable only in the gravitational term. This is called the Boussinesq approximation.

1.5 DIMENSIONLESS PARAMETERS

The dimensionless parameters can be thought of as measures of the relative importance of certain aspects of the flow. Some dimensionless parameters related to our study are discussed below:

Grashof number *Gr*

The flow regime in free convection is governed by the dimensionless Grashof number, which represent the ratio of the buoyancy force to the viscous forces acting on the fluid, and is defined as

$$Gr = \frac{g \beta L^3 \left(T_w - T_\infty\right)}{\nu^2}$$

where g is the acceleration due to gravity, β is the volumetric thermal expansion coefficient, T_w is the wall temperature, T_∞ is the ambient temperature, L is the characteristic length and ν is the

kinematics viscosity. The Grashof number Gr plays same role in free convection as the Reynolds number Re plays in forced convection. As such, the Grashof number provides the main criterion in determining whether the fluid flow is laminar or turbulent in free convection. For vertical plates, the critical value of the Grashof number is observed to be about 10^9. Therefore, the flow regime on a vertical plate becomes turbulent at Grashof numbers greater than 10^9.

Prandtl Number Pr

The relative thickness of the velocity and the thermal boundary layers is best described by the dimensionless parameter Prandtl number, defined as

Pr = Molecular diffusivity of momentum / Molecular diffusivity of heat = v/α

It is named after Ludwig Prandtl, who introduced the concept of boundary layer in 1904 and made significant contributions to boundary layer theory. The Prandtl numbers of fluids range from less than 0.01 for liquid metals to more than 100,000 for heavy oils. Note that the Prandtl number is in the order of 7 for water. The Prandtl numbers of gases are about 1, which indicates that both momentum and heat dissipate through the fluid at about the same rate. Consequently the thermal boundary layer is much thicker for liquid metals and much thinner for oils relative to the velocity boundary layer.

Nusselt Number Nu

The Nusselt number represents the enhancement of heat transfer through a fluid layer as a result of convection relative to conduction across the same fluid layer, and is defined as

$Nu = hL / k$

where k is the thermal conductivity of the fluid, h is the heat transfer coefficient and L is the characteristics length. The Nusselt number is named after Wilhelm Nusselt, who made significant contributions to convective heat transfer in the first half of the twentieth century, and it is viewed as the dimensionless convection heat transfer coefficient. The larger Nusselt number indicates a large temperature gradient at the surface and hence, high heat transfer by convection. A Nusselt number of $Nu = 1$, for a fluid layer represents heat transfer across the layer by pure conduction. To understand the physical significance of the Nusselt number, consider the following daily life problems. We remedy to forced convection whenever we want to increase the rate of heat transfer from a hot object. In free convection flow velocities are produced by the buoyancy forces hence there are no externally induced flow velocities.

1.6 MAIN OBJECTIVES OF THE WORK

The present study has focused on the development of a mathematical model and numerical techniques regarding the effects of natural convection flow around an adiabatic circular cylinder placed in a rectangular open cavity.

The specific objectives of the present research work are as follows:

- A mathematical model regarding the effect of natural convection flow around an adiabatic circular cylinder placed in a rectangular open cavity has developed.

- To visualize the fluid flow and temperature distribution inside the enclosure in terms of streamline and isotherm plots.

- The analytical model has numerically solved using finite element method.

- To investigate the effects of Grashof number and Prandtl number on the heat transfer characteristics (Nusselt number).

- To investigate the effects of diameter ratio of adiabatic cylinder on natural convection placed inside an open cavity.

- To carry out the validation of the present finite element model by investigating the effect of natural convection heat transfer in a rectangular open cavity.

- To examine the effects of inclination angles of the enclosure on the heat transfer characteristics.

LITERATURE REVIEW

Natural convection in open cavities has received considerable attention because of its importance in several thermal engineering problems, for example, in the design of electronic devices, solar thermal receivers, uncovered flat plate solar collectors having rows of vertical strips, geothermal reservoirs, etc. During the past two decades, several experiments and numerical calculations have been presented for describing the phenomenon of natural convection in open cavities. Those studies have been focused to study the effect on flow and heat transfer for different Rayleigh numbers, aspect ratios, and tilt angles.

Natural convection in an air filled, differentially heated, inclined square cavity with a diathermal partition placed at the middle of its cold wall was numerically studied for Rayleigh numbers 10^3 to 10^5. It was observed that due to suppression of convection, heat transfer reductions up to 47 percent in comparison to the cavity without partition observed by Frederick (1991). Laminar natural convection and conduction in enclosures with multiple vertical partitions are studied theoretically by Kangni et al. (2003). The study covers Rayleigh number Ra in the range 10^3-10^7, Pr = 0.72 (air) aspect ratio 5–20, cavity width 0.1–0.9 and partition thickness 0.01–0.1. They found that the heat transfer decreases with increasing partition number at high Rayleigh number for all conductivity ratios Kr and heat transfer decreases with increasing partition thickness C at all Ra except in the conduction regime where the effect is negligibly small. The offender partitions are less effective in decreasing the heat transfer. Nusselt number is also a decreasing function in the aspect ratio. Tasnim and Collins (2004) determined the effect of a horizontal baffle placed on hot (left) wall of a differentially heated square cavity. It has been found that adding baffle on the hot wall can increase the rate of heat transfer by as much as 31.46 percent compared with a wall without baffle for Ra = 104. When Ra = 105 the increase in heat transfer is 15.3 percent for the same baffle length and the increases in heat transfer is 19.73 percent, when the longest baffle is attached at the middle of the cavity. Bilgen and Oztop (2005) studied numerically the steady-state heat transfer by natural convection in partially open inclined square cavities.

Natural convection in fluid-filled rectangular enclosures has received considerable attention over the past several years due to the wide variety of applications that involve natural convection processes. These applications span such diverse fields as solar energy collection, nuclear reactor operation and safety, the energy efficient design of building, room, and machinery, waste disposal, and fire prevention and safety. The oscillation-induced heat transport has been studied by a number of researchers due to its many industrial applications, such as bioengineering,

chemical engineering, and so forth. Kuhn and Oosthuizen (1987) numerically studied unsteady natural convection in a partially heated rectangular cavity. They concluded that as the heated location moves from the top to the bottom, the Nusselt number increases up to a maximum and then decreases. Lakhal et al. (1999) studied the transient natural convection in a square cavity partially heated from side. In the first, the temperature is varied sinusoidal with time while in the second; it varies with a pulsating manner. The results showed that the mean values of heat transfer and flow intensity are considerably different with those obtained in stationary regime. Le Quere et al (1981) investigated the effect on the flow field and heat transfer of the Grashof number as it varied from 10^4 to 3×10^7; the temperature difference between the cavity walls and ambient changed from 50 to 500 K, the aspect ratio varied between 0.5 and 2, and the inclination angle of the cavity was modified from 0 to $45°$ (for $0°$ the wall opposite the aperture was vertical and the angles were taken clockwise). The results of the paper showed that the Nusselt number diminished with the increase in the inclination angle, and that the unsteadiness in the flow takes place for values of the Grashof number greater than 10^6 and inclination angles of $0°$. Showole and Tarasuk (1993) investigated, experimentally and numerically, the natural steady state convection in a two dimensional isothermal open cavity. They obtained experimental results for air, varying the Rayleigh number from 10^4 to 5.5×10^5, cavity aspect ratios of 0.25, 0.5 and 1.0, and inclination angles of 0, $30°$, $45°$ and $60°$ (for $0°$, the wall opposite the aperture was horizontal and the angles were taken clockwise). The numerical results were calculated for Rayleigh numbers between 10^4 and 5.5×10^5, inclination angles of 0 and $45°$, and an aspect ratio equal to one. The results showed that, for all Rayleigh numbers, the first inclination of the cavity caused a significant increase in the average heat transfer rate, but a further increase in the inclination angle caused very little increase in the heat transfer rate. Another result observed was that, for $0°$, two symmetric counter rotating eddies were formed, while at inclination angles greater than $0°$, the symmetric flow and temperature patterns disappear.

Mohamad (1995) studied numerically the natural convection in an inclined two-dimensional open cavity with one heated wall opposite the aperture and two adiabatic walls. The author analyzed the influence on fluid flow and heat transfer, with the inclination angle in the range $10°$-$90°$ (for $90°$ the wall opposite the aperture was vertical and the angles were taken clockwise), the Rayleigh number from 10^3 to 10^7, and the aspect ratio between 0.5 and 2. The study concludes that the inclination angle did not have a significant effect on the average Nusselt number from the isothermal wall, but a substantial one on the local Nusselt number. Polat and Bilgen (2002) made a numerical study of the conjugate heat transfer by conduction and natural convection in an inclined, open shallow cavity with a uniform heat flux in the wall opposite to the aperture. The parameters studied were: the Rayleigh number from 10^6 to 10^{12}, the conductivity ratio from 1 to 60, the cavity aspect ratio from 1 to 0.125, the dimensionless wall thickness from 0.05 to 0.20,

and the inclination angle from 0 to 45° from the horizontal (for 0°, the wall opposite the aperture was vertical and the angles were taken counterclockwise).

Le Quere et al (1981) investigated thermally driven laminar natural convection in enclosures with isothermal sides, one of which facing the opening. They used primitive variables and finite difference expressions suitable for treating problems with large temperature and density variations. The computational domain was an enlarged domain comprising a square open cavity and a far field surrounding it. Penot (1982) studied a similar problem using stream function-vorticity formulation. He also used an enlarged computational domain similar to that of Le Quere et al (1981) with approximate boundary conditions. Chan and Tien (1985) studied numerically a square open cavity, which had an isothermal vertical heated side facing the opening and two adjoining adiabatic horizontal sides. The boundary conditions at far field were approximated to obtain satisfactory solutions in the open cavity. Chan and Tien (1985) studied numerically shallow open cavities and also made a comparison study using a square cavity in an enlarged computational domain. They found that for a square open cavity having an isothermal vertical side facing the opening and two adjoining adiabatic horizontal sides, satisfactory heat transfer results could be obtained, especially at high Rayleigh numbers. In a similar way, Mohamad (1995) studied inclined open square cavities, by considering a restricted computational domain. Different from those by Chan and Tien (1985), gradients of both velocity components were set to zero at the opening plane. It was found that heat transfer was not sensitive to inclination angle and the flow was unstable at high Rayleigh numbers and small inclinations angles. Polat and Bilgen (2002) studied numerically inclined open shallow cavities in which the side facing the opening was heated by constant heat flux, two adjoining walls were insulated and the opening was in contact with a reservoir at constant temperature and pressure. The computational domain was restricted to the cavity.

The finite element method is one of the numerical methods that have received popularity due to its capability for solving complex structural problems (Cook, 1989, Zienkiewicz, 1991). The method has been extended to solve problems in several other fields such as in the field of heat transfer (Lewis et al., 1996, Dechaumphai, 1999), electromagnetics (Jini, 1993), biomechanics (Gallagher et al., 1982), etc. In spite of the great success of the method in these fields, its application to fluid mechanics is still under intensive research. This is due to the fact that the governing differential equations for general flow problems consist of several coupled equations which are inherently nonlinear. Accurate numerical solutions thus require a vast amount of computer time and data storage. One-way to minimize the amount of computer time and data storage used is to employ an adaptive meshing technique (Dechaumphai, 1995, Peraire et al., 1987) The technique places small elements in the regions of large change in the solution

gradients to increase solution accuracy, and at the same time, uses large elements in the other regions to reduce the computational time and computer memory.

Goutam Saha et al (2007) studied a numerical simulation of two-dimensional laminar steady-state natural convection in a square tilt open cavity has been numerically studied. The opposite wall to the aperture is kept at either constant surface temperature or constant heat flux, while the surrounding fluid interacting with the aperture is maintained at an ambient temperature. The two remaining walls are assumed to be adiabatic. The fluid concerned is air with Prandtl number fixed at 0.71. The governing mass, momentum and energy equations are expressed in a normalized primitive variables formulation. A finite element method for steady-state incompressible natural convection flows has been developed. The streamlines and isotherms are produced, heat transfer characteristics is obtained for Rayleigh numbers from 10^3 to 10^6 and for an inclination angles of the cavity ranges from $0°$ to $60°$.

In experimental studies of Ozoe et al. (1975), Arnold et al. (1976), Linthorst et al. (1981) and Hamady et al. (1989) found as the tilt angle changes from $0°$ to $90°$, the heat transfer decreases until a minimum point is reached, and then gradually increases again and the minimum point occurs at the angle where flow changes its mode from the three-dimensional roll pattern caused by the thermal instability to the two-dimensional circulation caused by the hydrodynamic effect. Most of these experimental researches only studied cavities with small to medium aspect ratios, with the maximum aspect ratio 15.5. In the study of Elsherbiny et al. (1982), six aspect ratios between 5 and 110 were examined experimentally to find the influence of the tilt angle and the aspect ratio on the heat transfer rate. A correlation for tilt angle $60°$ was developed, and a suggestion of a straight-line interpolation between $60°$ and $90°$ was proposed. A lot of numerical studies were also performed. Most of them are two dimensional and only studied flow in an inclined square cavity, such as Ozoe et al. (1974), Chen et al. (1985), Kuyper et al. (1992) and Zhong et al. (1985). However, these two-dimensional numerical studies could not work well at small tilt angles close to horizontal position. In the recent paper of Soong et al. (1996), the same model of square cavity from Ozoe et al. (1974) was studied with the imperfect constant wall temperature boundary conditions, and the results showed good agreement with the experimental curve even at small tilt angles.

In the present thesis a numerical simulation of two-dimensional laminar steady-state natural convection in a rectangular open cavity has numerically studied. An adiabatic circular cylinder is placed at the center of the cavity and the opposite wall to the aperture is heated by a constant heat flux. The top and bottom walls are kept at the constant temperature. The fluid is concerned with Prandtl number at 0.72, 1.0 and 7.0. The governing mass, momentum and energy equations are expressed in a normalized primitive variables formulation. In this thesis, a finite element method for steady-state incompressible natural convection flows has been developed. The streamlines

13

and isotherms are produced, heat transfer characteristics is obtained for Grashof numbers from 10^3 to 10^6 and for an inclination angles of the cavity ranges from 0° to 45°. The results show that the Nusselt number increases with the Grashof numbers. Also the Nusselt number has changed substantially with the inclination angle of the cavity while better thermal performance is also sensitive to the boundary condition of the heated wall.

MODEL DESCRIPTION

3.1 PHYSICAL MODEL

The heat transfer and the fluid flow in a two-dimensional open rectangular cavity of length L was considered, as shown in the schematic diagram of figure3.1. The opposite wall to the aperture was first kept to constant heat flux q, while the surrounding fluid interacting with the aperture was maintained to an ambient temperature T_a. The top and bottom walls were kept to constant temperature T_h. The remaining circular cylinder was assumed to be adiabatic. The fluid was assumed with Prandtl number (Pr = 0.72, 1.0, 7.0) and Newtonian, and the fluid flow is considered to be laminar. The properties of the fluid were assumed to be constant.
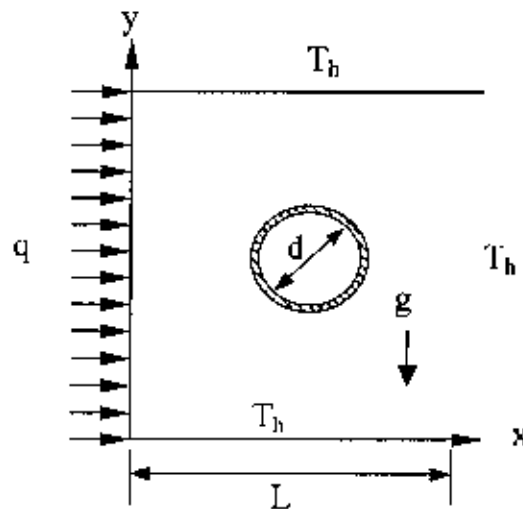
Figure-3.1. Schematic diagram of the physical system.

3.2 MATHEMATICAL MODEL

Natural convection is governed by the differential equations expressing conservation of mass, momentum and energy. The present flow is considered steady, laminar, incompressible and two-dimensional. The viscous dissipation term in the energy equation is neglected. The Boussinesq approximation is invoking for the fluid properties to relate density changes to temperature changes, and to couple in this way the temperature field to the flow field. The governing equations for steady natural convection flow can be written as:

$$\frac{\partial u}{\partial x} + \frac{\partial u}{\partial y} = 0 \tag{1}$$

$$u\frac{\partial u}{\partial x} + v\frac{\partial u}{\partial y} = -\frac{1}{\rho}\frac{\partial p}{\partial x} + \gamma \left(\frac{\partial^2 u}{\partial x^2} + \frac{\partial^2 u}{\partial y^2} \right) + g\ \beta\ (T - T_\infty)\ \sin\Phi \tag{2}$$

$$u\frac{\partial v}{\partial x} + v\frac{\partial v}{\partial y} = -\frac{1}{\rho}\frac{\partial p}{\partial y} + \gamma \left(\frac{\partial^2 v}{\partial x^2} + \frac{\partial^2 v}{\partial y^2} \right) + g\ \beta\ (T - T_\infty)\ \cos\Phi \tag{3}$$

$$u\frac{\partial T}{\partial x} + v\frac{\partial T}{\partial y} = \alpha \left(\frac{\partial^2 T}{\partial x^2} + \frac{\partial^2 T}{\partial y^2} \right) \tag{4}$$

The boundary conditions used are:

$$u(x,0) = u(0,y) = u(x,L) = 0$$
$$v(x,0) = v(0,y) = v(x,L) = 0$$

$$\frac{\partial \theta}{\partial y}(x,\ 0) = \frac{\partial \theta}{\partial y}(x,\ L) = 0$$

$$\frac{\partial u}{\partial x}(L,\ y) = \frac{\partial v}{\partial x}(L,\ y) = 0$$

where x and y are the distances measured along the horizontal and vertical directions, respectively; u and v are the velocity components in the x- and y-direction, respectively; T denotes the temperature; γ and α are the kinematic viscosity and the thermal diffusivity, respectively; p is the pressure and ρ is the density; θ_h and θ_∞ are the constant and ambient temperatures respectively. The governing equations in non-dimensional form are written as follows:

16

$$\frac{\partial U}{\partial X} + \frac{\partial V}{\partial Y} = 0$$

(5)

$$U\frac{\partial U}{\partial X} + V\frac{\partial U}{\partial Y} = -\frac{\partial P}{\partial X} + \frac{1}{\sqrt{Gr}}\left(\frac{\partial^2 U}{\partial X^2} + \frac{\partial^2 U}{\partial Y^2}\right) + \theta \ \sin\Phi$$

(6)

$$U\frac{\partial V}{\partial X} + V\frac{\partial V}{\partial Y} = -\frac{\partial P}{\partial Y} + \frac{1}{\sqrt{Gr}}\left(\frac{\partial^2 V}{\partial X^2} + \frac{\partial^2 V}{\partial Y^2}\right) + \theta \cos\Phi$$

(7)

$$U\frac{\partial \theta}{\partial X} + V\frac{\partial \theta}{\partial Y} = \frac{1}{Pr\sqrt{Gr}}\left(\frac{\partial^2 \theta}{\partial X^2} + \frac{\partial^2 \theta}{\partial Y^2}\right)$$

(8)

with the boundary conditions

$$U(X,\ 0) = U(X,\ 1) = U(0,\ Y) = 0,$$

$$V(X,\ 0) = V(X,\ 1) = V(0,\ Y) = 0,$$

$$\frac{\partial \theta}{\partial Y}(X,\ 0) = \frac{\partial \theta}{\partial Y}(X,\ 1) = 0$$

$$\frac{\partial U}{\partial X}(1,\ Y) = \frac{\partial V}{\partial X}(1,\ Y) = 0$$

$$\frac{\partial \theta}{\partial X}(0,\ Y) = -1$$

Equations (5)-(8) were normalized using the following dimensionless scales:

$$X = \frac{x}{L}, \ Y = \frac{y}{L}, \ U = \frac{u}{U_0}, \ V = \frac{v}{U_0},$$

$$P = \frac{p - p_\infty}{\rho U_0^2}, \ T = \frac{\theta - \theta_\infty}{\Delta t}, \quad = \frac{\nu}{\alpha}, \ Gr = \frac{g \, \beta \, \Delta T \, L^3}{\nu^2}, \ dr = \frac{D}{L}$$

$$\Delta t = \left(\theta_h - \theta_\infty \right)$$

$$\Delta t = \frac{q L}{k}$$

Here Gr and Pr are Grashof and Prandtl numbers, respectively. The Grashof number represents the ratio of the buoyancy force to the viscous force acting on the fluid. The reference velocity U_0 is related to the buoyancy force term and is defined as

$$U_0 = \sqrt{g \beta L \left(\theta_h - \theta_\infty \right)} \ .$$

The Nusselt number (Nu) is one of the important dimensionless parameters to be computed for heat transfer analysis in natural convection flow. Also the Nusselt number for free convection is a function of the Grashof number only. The local Nusselt number can be obtained from the temperature field by applying

$$Nu = -\frac{1}{\theta(0, Y)}$$

and the average or overall Nusselt number was calculated by integrating the temperature gradient over the heated wall as

$$Nu_{av} = \int_0^1 \frac{1}{\theta(0, Y)} dY$$

3.3 COMPUTATIONAL DETAILS

The governing equations in fluid dynamics and heat transfer, including conservation forms of the Navier-Stokes system of equations as derived from the first law of thermodynamics, expressed in terms of the control volume / surface integral equations, which represent various physical phenomena. To visualize these thermo fluid flow scenarios, an approximate numerical solution is needed, which can be obtained by the CFD (Computational Fluid Dynamics) code. The partial differential equations of fluid mechanics and heat transfer are discretized in order to obtain a system of approximate algebraic equations, which then can be solved on a computer. The approximations are applied to small domains in space and/ or time so the numerical solution provides results at discrete locations in space and time. Much accuracy of experimental data depends on the quality of the tools used; the accuracy of numerical solution is dependent on the quality of discretization used. CFD computation involves the creation of a set numbers that constitutes a realistic approximation of a real life system. The outcome of computation process improves the understanding of the behavior of a system. Thereby, engineers need CFD codes that can produce physically realistic results with good accuracy in simulations with finite grids. Contained within the broad field of computational fluid dynamics are activities that cover the range from the automation of well established engineering design methods to the use of detailed solutions of the Navier-Stokes equations as substitutes for experimental research into the nature of complex flows. CFD have been used for solving wide range of fluid dynamics problem. It is more frequently used in fields of engineering where the geometry is complicated or some important feature that cannot be dealt with standard methods. The complete Navier-Stokes equations are considered to be the correct mathematical description of the governing equations of fluid motion. The most accurate numerical computations in fluid dynamics come from solving the Navier-Stokes equations. The equations represent the conservation of mass and momentum.

There are several discretization methods available for the high performance numerical computation in CFD.

- Finite volume method (FVM)

- Finite element method (FEM)

- Finite difference method (FDM)

- Boundary element method (BEM)

- Boundary volume method (BVM)

In the present numerical computation, Galerkin Finite Element Method (FEM) is used.

3.4 FINITE ELEMENT METHOD

The finite element method (FEM) is a powerful computational technique for solving problems that are described by partial differential equations. The basic idea of the finite element method is the domain is broken into a set of finite elements that are generally triangular or quadrilaterals. The distinguishing feature of FE methods is that the equations are multiplied by a weight function before they are integrated over the entire domain. In the simplest FE methods, the solution is approximated by a linear shape function within each element in a way that guarantees continuity of the solution across element boundaries. Such a function can be constructed from its values at the corners of the elements. The weight function may be the same or different form. This approximation is then substituted into the weighted integral of the conservation law the equations to be solved are derived by requiring the derivative of the integral with respect to each nodal value to be zero; this corresponds to selecting the best solution within the set of allowed functions. The result is a set of nonlinear algebraic equations.

Mathematical model of physical phenomena may be ordinary or partial differential equations, which have been the subject of analytical and numerical investigations. Analytical solutions of these equations involve closed form expressions that give us the variation of the dependent variables continuously throughout the domain. On the other hand, for most of these equations there are no available analytical methods to find their solutions. In contrast, there are available numerical methods to solve these equations. Numerical solutions of these equations can give answers at only discrete points in the domain. In addition, numerical methods give us approximate solution of these differential equations. To obtain an approximate solution numerically, one has to use a discretization technique that approximates the differential equations by a system of algebraic equations at only discrete points in the domain, which can then be solved on a computer.

The first step to numerically solve a mathematical model of physical phenomena is its numerical discretization. This means that each component of the differential equations is transformed into a "numerical analogue" which can be represented in the computer and then processed by a

computer program, built on some algorithm. There are many different methodologies were devised for this purpose in the past and the development still continues. In this thesis the finite element method (FEM) has been used to solve the differential equations.

3.5 THE REASON FOR FINITE-ELEMENT SOLUTION

The analysis of flow and heat transfer in thermodynamics can be performed either theoretically or by experimental means. Experimental investigation of such problem could not gain that much popularity in the field of thermodynamics because of their limited flexibility and applications. For every change of geometry body and boundary condition, it needs separate investigation, involving separate experimental requirement/ arrangement, which, in turn makes it unattractive, especially, from the time involved as well as economical point of views. The theoretical investigation, on the other hand, can be carried out either by analytical approach or by numerical approach. The analytical methods of solution are not of much help in solving the practical problems. This is mainly due to the very involvement of a large number of variables, complex geometrical bodies and boundary conditions, and arbitrary boundary shapes. General closed form solutions can be obtained only for very ideal cases and the results obtained for a particular problem, usually with uniform boundary conditions. For two-dimensional thermodynamics problems, mathematical model involve partial differential equations are required to be solved simultaneously with some boundary conditions. Therefore, there are no alternatives except the numerical methods for the solution of the problems of practical interest. In the field of numerical analysis, the major numerical methods in use are the method of finite difference (FD), finite volume (FV) and finite element (FE).

Finite element method is an ideal numerical approach for solving a system of partial differential equations. The finite element method produces equations for each element independently of all other elements. Only when the equations are collected together and assembled into a global matrix are the interactions between elements taken into account. Despite these ideal characteristics, the finite element method dominates in most of the computational fluid dynamics. The present research is an attempt to bring the FE technique again into light through a novel formulation of two dimensional incompressible thermal flow problems. As the formulation establishes a priority of finite element technique over the FD and FV method, the philosophy and approach of the three methods are recapitulated here in brief. The finite difference method relies on the philosophy that the body is in one single piece but the parameters are evaluated only at some selected points within the body, satisfying the governing differential equations approximately, where as the finite volume method relies on the philosophy that the body is divided into a finite number of control volumes, On the other hand, in the finite element method,

the body is divided into a number of elements. The relative advantages and disadvantages of the finite element method is shown below:

Finite Element Method

Advantages

a) Finite element method works when all other methods fail.

b) It is very good in managing complex geometrical bodies and boundaries.

c) There are many commercial packages such as ANSYS, FEMLAB for analyzing practical problems.

Disadvantages

a) The body is not in one piece, but it is an assemblage of elements connected only at nodes.

b) Variations of parameters over individual elements are assumed to be simple like polynomial of limited order.

c) Finite element solution is highly dependent on the element type.

Accurate and reliable prediction of complex geometry is of great importance to meet the severe demand of greater reliability as well as economic challenge. It is noted that these complex geometries occurs most frequently in CFD. Presented methods have a common feature: they generate equations for the values of the unknown functions at a finite number of points in the computational domain. But there are also several differences. The finite difference and the finite volume methods generate numerical equations at the reference point based on the values at neighboring points. The finite element method takes care of boundary conditions of Neumann type while the other two methods can easily apply to the Dirichlet conditions. The finite difference method could be easily extended to multidimensional spatial domains if the chosen grid is regular (the cells must look cuboids, in a topological sense). The grid indexing is simple but some difficulties appear for the domain with a complex geometry. For the finite element method there are no restrictions on the connection of the elements when the sides (or faces) of the elements are correctly aligned and have the same nodes for the neighboring elements. This flexibility allows us to model a very complex geometry The finite volume method could also use irregular grids like the grids for the finite element methods, but keeps the simplicity of writing the equations like that for the finite difference method. Of course, the presence of a complex geometry slows down the computational programs. Another benefit of the finite element method is that of the specific mode to deduce the equations for each element that are then assembled. Therefore, the addition of new elements by refinement of the existing ones is not a major

22

problem. For the other methods, the mesh refinement is a major task and could involve the rewriting of the program. But for all the methods used for the discrete analogue of the initial equation, the obtained system of simultaneous equations must be solved. That is why, the present work emphasizes the use of finite element techniques to solve flow and heat transfer problems. The details of this method are explained in the following section.

3.6 FEM FOR VISCOUS INCOMPRESSIBLE FLOW

Viscous incompressible thermal flows have been the subject of this investigation. The problem is relatively complex due to the coupling between the energy equation and the Navier-Stokes equations that govern the fluid motion. These equations comprise a set of coupled nonlinear partial differential equations that is difficult to solve especially with complicated geometries and boundary conditions. The finite element method is one of the numerical methods that have received popularity due to its capability for solving complex structural problems. The method has been extended to solve problems in several other fields such as in the field of heat transfer, computational fluid dynamics, electromagnetic, biomechanics etc. In spite of the great success of the method in these fields, its application to fluid mechanics, particularly to convective viscous flows, is still under intensive research. This is due to the fact that the governing partial differential equations for general flow problems consist of several coupled equations that are naturally nonlinear. Accurate numerical solutions thus require a vast amount of computer time and data storage. One-way to minimize the amount of computer time and data storage used is to employ an adapting meshing technique. The technique places small elements in the regions of large change in the solution gradient to increase solution accuracy, and at the same time, uses large elements in the other regions to reduce the computational time and computer memory.

As the first step toward accurate flow solutions using the adaptive meshing techniques, this chapter develops a finite element formulation suitable for analysis of general viscous incompressible thermal flow problems. The formulation evaluated in this chapter will be used with the adaptive meshing technique in the future. The chapter starts from the Navier-Stokes equations together with the energy equation to derive the corresponding finite element equations. The computational procedure used in the development of the computer program is described.

The major steps involved in finite element analysis of a typical problem are:

- Discretization of the domain into a set of finite elements (mesh generation).
- Weighted-integral or weak formulation of the differential equation to be analyzed.
- Development of the finite element model of the problem using its weighted-integral or weak form.
- Assembly of finite elements to obtain the global system of algebraic equations.

- Imposition of boundary conditions.

- Solution of equations.

- Post-computation of solution and quantities of interest.

3.7 NUMERICAL PROCEDURE

The numerical procedure used to solve the governing equations for the present work is based on the Galerkin weighted residual method of finite-element formulation. The non-linear parametric solution method is chosen to solve the governing equations. This approach will result in substantially fast convergence assurance. A non-uniform triangular mesh arrangement is implemented in the present investigation especially near the walls to capture the rapid changes in the dependent variables.

The velocity and thermal energy equations (5)-(8) result in a set of non-linear coupled equations for which an iterative scheme is adopted. To ensure convergence of the numerical algorithm the following criteria is applied to all dependent variables over the solution domain

$$\sum \left| \phi_{ij}^{m} - \phi_{ij}^{m-1} \right| \leq 10^{-5}$$

where ϕ represents a dependent variable U, V, P, and T; the indexes i, j indicate a grid point; and the index m is the current iteration at the grid level. The six node triangular element is used in this work for the development of the finite element equations. All six nodes are associated with velocities as well as temperature; only the corner nodes are associated with pressure. This means that a lower order polynomial is chosen for pressure and which is satisfied through continuity equation The velocity component and the temperature distributions and linear interpolation for the pressure distribution according to their highest derivative orders in the differential Eqs (5)-(8) as

$$U(X, Y) = N_\alpha U_\alpha \tag{9}$$

$$V(X, Y) = N_\alpha V_\alpha \tag{10}$$

$$\theta(X, Y) = N_\alpha \theta_\alpha \tag{11}$$

$$P(X, Y) = H_\lambda P_\lambda \tag{12}$$

where α = 1, 2, ..., 6; λ= 1, 2, 3; N_α are the element interpolation functions for the velocity components and the temperature, and H_λ are the element interpolation functions for the pressure.

To derive the finite element equations, the method of weighted residuals (Zienkiewicz, 1991) is applied to the continuity Eq. (5), the momentum Eqs (6)-(7), and the energy Eq. (8), we get

$$\int_A N_\alpha \left(\frac{\partial U}{\partial X} + \frac{\partial V}{\partial Y} \right) dA = 0 \tag{13}$$

$$\int_A N_\alpha \left(U \frac{\partial U}{\partial X} + V \frac{\partial U}{\partial Y} \right) dA = - \int_A H_\lambda \left(\frac{\partial P}{\partial X} \right) dA$$
$$+ \frac{1}{\sqrt{Gr}} \int_A N_\alpha \left(\frac{\partial^2 U}{\partial X^2} + \frac{\partial^2 U}{\partial Y^2} \right) dA + \int_A N_\alpha (\sin \Phi) \theta dA \tag{14}$$

$$\int_A N_\alpha \left(U \frac{\partial V}{\partial X} + V \frac{\partial V}{\partial Y} \right) dA = - \int_A H_\lambda \left(\frac{\partial P}{\partial Y} \right) dA$$
$$+ \frac{1}{\sqrt{Gr}} \int_A N_\alpha \left(\frac{\partial^2 V}{\partial X^2} + \frac{\partial^2 V}{\partial Y^2} \right) dA + \int_A N_\alpha (\cos \Phi) \theta dA \tag{15}$$

$$\int_A N_\alpha \left(U \frac{\partial \theta}{\partial X} + V \frac{\partial \theta}{\partial Y} \right) dA = \frac{1}{Pr \sqrt{Gr}} \int_A N_\alpha \left(\frac{\partial^2 \theta}{\partial X^2} + \frac{\partial^2 \theta}{\partial Y^2} \right) dA \tag{16}$$

where A is the element area. Gauss's theorem is then applied to Eqs (14)-(16) to generate the boundary integral terms associated with the surface tractions and heat flux. Then Eqs (14)-(16) become,

$$\int_A N_\alpha \left(U \frac{\partial U}{\partial X} + V \frac{\partial U}{\partial Y} \right) dA + \int_A H_\lambda \left(\frac{\partial P}{\partial X} \right) dA +$$
$$\frac{1}{\sqrt{Gr}} \int_A \left(\frac{\partial N_\alpha}{\partial X} \frac{\partial U}{\partial X} + \frac{\partial N_\alpha}{\partial Y} \frac{\partial U}{\partial Y} \right) dA - \int_A \sin \Phi N_\alpha \theta dA = \int_{S_0} N_\alpha S_x dS_0 \tag{17}$$

$$\int_A N_\alpha \left(U \frac{\partial V}{\partial X} + V \frac{\partial V}{\partial Y} \right) dA + \int_A H_\lambda \left(\frac{\partial P}{\partial Y} \right) dA +$$
$$\frac{1}{\sqrt{Gr}} \int_A \left(\frac{\partial N_\alpha}{\partial X} \frac{\partial V}{\partial X} + \frac{\partial N_\alpha}{\partial Y} \frac{\partial V}{\partial Y} \right) dA - \int_A \cos \Phi N_\alpha \theta dA = \int_{S_0} N_\alpha S_y dS_0 \tag{18}$$

$$\int_A N_\alpha \left(U \frac{\partial \theta}{\partial X} + V \frac{\partial \theta}{\partial Y} \right) dA + \frac{1}{Pr \sqrt{Gr}} \int_A \left(\frac{\partial N_\alpha}{\partial X} \frac{\partial \theta}{\partial X} + \frac{\partial N_\alpha}{\partial Y} \frac{\partial \theta}{\partial Y} \right) dA$$
$$= \int_{S_w} N_\alpha q_w dS_w \tag{19}$$

Here (14)-(15) specifying surface tractions (S_x, S_y) along outflow boundary S_0 and (16) specifying velocity components and fluid temperature or heat flux that flows into or out from domain along wall boundary S_w. Substituting the element velocity component distributions, the

temperature distribution, and the pressure distribution from Eqs (9)-(12), the finite element equations can be written in the form,

$$K_{\alpha\beta}x\, U_\beta + K_{\alpha\beta}y\, V_\beta = 0 \tag{20}$$

$$
\begin{aligned}
& K_{\alpha\beta\gamma'}U_\beta U_\gamma + K_{\alpha\beta\gamma'}V_\gamma U_\gamma + M_{\alpha\mu'}P_\mu + \frac{1}{\sqrt{Gr}}\left(S_{\alpha\beta^{xx}} + S_{\alpha\beta^{yy}}\right)U_\beta \\
& - \sin\Phi\; K_{\alpha\beta}\theta_\beta = Q_{\alpha''}
\end{aligned} \tag{21}
$$

$$
\begin{aligned}
& K_{\alpha\beta\gamma'}U_\beta V_\gamma + K_{\alpha\beta\gamma'}V_\gamma V_\gamma + M_{\alpha\mu'}P_\mu + \frac{1}{\sqrt{Gr}}\left(S_{\alpha\beta^{xx}} + S_{\alpha\beta^{yy}}\right)V_\beta \\
& - \cos\Phi\; K_{\alpha\beta}\theta_\beta = Q_{\alpha'}
\end{aligned} \tag{22}
$$

$$
K_{\alpha\beta\gamma'}U_\beta\theta_\gamma + K_{\alpha\beta\gamma'}V_\beta\theta_\gamma + \frac{1}{Pr\sqrt{Gr}}\left(S_{\alpha\beta^{xx}} + S_{\alpha\beta^{yy}}\right)\theta_\beta = Q_{\alpha^T} \tag{23}
$$

where the coefficients in element matrices are in the form of the integrals over the element area and along the element edges S_0 and S_w as,

$$K_{\alpha\beta}x = \int_A N_\alpha N_{\beta,x}\,dA , \tag{24a}$$

$$K_{\alpha\beta}y = \int_A N_\alpha N_{\beta,y}\,dA , \tag{24b}$$

$$K_{\alpha\beta\gamma}x = \int_A N_\alpha N_\beta N_{\gamma,x}\,dA , \tag{24c}$$

$$K_{\alpha\beta\gamma}y = \int_A N_\alpha N_\beta N_{\gamma,y}\,dA , \tag{24d}$$

$$K_{\alpha\beta} = \int_A N_\alpha N_\beta\,dA , \tag{24e}$$

$$S_{\alpha\beta}xx = \int_A N_{\alpha,x} N_{\beta,x}\,dA , \tag{24f}$$

$$S_{\alpha\beta}yy = \int_A N_{\alpha,y} N_{\beta,y}\,dA , \tag{24g}$$

$$M_{\alpha\mu}x = \int_A H_\alpha H_{\mu,x}\,dA , \tag{24h}$$

$$M_{\alpha\mu}y = \int_A H_\alpha H_{\mu,y}\,dA , \tag{24i}$$

$$Q_\alpha u = \int_{S_0} N_\alpha S_x dS_0 , \qquad\qquad (24j)$$

$$Q_\alpha v = \int_{S_0} N_\alpha S_y dS_0 , \qquad\qquad (24k)$$

$$Q_\alpha \theta = \int_{S_w} N_\alpha \; q_w dS_w . \qquad\qquad (24l)$$

These element matrices are evaluated in closed-form ready for numerical simulation. Details of the derivation for these element matrices are omitted herein for brevity.

The derived finite element equations, Eqs (20)-(23), are nonlinear. These nonlinear algebraic equations are solved by applying the Newton-Raphson iteration technique (Dechaumphai, 1999) by first writing the unbalanced values from the set of the finite element Eqs (20)-(23) as,

$$F_\alpha p = K_{\alpha\beta} x \, U_\beta + K_{\alpha\beta} y \, V_\beta \qquad\qquad (25a)$$

$$F_{\alpha^x} = K_{\alpha\beta\gamma^x} U_\beta U_\gamma + K_{\alpha\beta\gamma^y} V_\gamma U_\gamma + M_{\alpha\mu^x} P_\mu +$$
$$\frac{1}{\sqrt{Gr}} \; (S_{\alpha\beta^{xx}} + S_{\alpha\beta^{yy}}) \; U_\beta - \; \sin\Phi \; K_{\alpha\beta}\theta_\beta - Q_{\alpha^x} \qquad (25b)$$

$$F_{\alpha^y} = K_{\alpha\beta\gamma^x} U_\beta V_\gamma + K_{\alpha\beta\gamma^y} V_\gamma V_\gamma + M_{\alpha\mu^y} P_\mu$$
$$+ \frac{1}{\sqrt{Gr}} (S_{\alpha\beta^{xx}} + S_{\alpha\beta^{yy}}) V_\beta - \cos\Phi \; K_{\alpha\beta}\theta_\beta - Q_{\alpha^y} \qquad (25c)$$

$$F_{\alpha^T} = K_{\alpha\beta\gamma^x} U_\beta \theta_\gamma + K_{\alpha\beta\gamma^y} V_\beta \theta_\gamma +$$
$$\frac{1}{\Pr\sqrt{Gr}} \left(S_{\alpha\beta^{xx}} + S_{\alpha\beta^{yy}}\right) \; \theta_\beta - Q_{\alpha^T} \qquad (25d)$$

This leads to a set of algebraic equations with the incremental unknowns of the element nodal velocity components, temperatures, and pressures in the form,

$$\begin{bmatrix} K_{uu} & K_{uv} & K_{u\theta} & K_{up} \\ K_{vu} & K_{vv} & K_{v\theta} & K_{vp} \\ K_{\theta u} & K_{\theta v} & K_{\theta\theta} & 0 \\ K_{pu} & K_{pv} & 0 & 0 \end{bmatrix} \begin{Bmatrix} \Delta u \\ \Delta v \\ \Delta\theta \\ \Delta p \end{Bmatrix} = - \begin{Bmatrix} F_{\alpha^x} \\ F_{\alpha^y} \\ F_{\alpha^\theta} \\ F_{\beta^u} \end{Bmatrix} \qquad (26)$$

where

$$K_{uu} = K_{\alpha\beta\gamma^x} U_\gamma + K_{\alpha\gamma\beta^x} U_\gamma + K_{\alpha\beta\gamma^y} V_\beta + \frac{1}{\sqrt{Gr}} \left(S_{\alpha\beta^{xx}} + S_{\alpha\beta^{yy}}\right)$$

$$K_{uv} = K_{\alpha\beta\gamma}{}^y U\gamma,$$

$$K_{u\theta} = -\sin\Phi \; K_{\alpha\beta},$$

$$K_{up} = M_{\alpha\mu}{}^x,$$

$$K_{vu} = K_{\alpha\beta\gamma}{}^x V\gamma,$$

$$K_{vv} = K_{\alpha\beta\gamma'} U_\beta + K_{\alpha\gamma\beta'} V_\gamma + K_{\alpha\beta\gamma'} V_r + \frac{1}{\sqrt{Gr}}\left(S_{\alpha\beta^{xx}} + S_{\alpha\beta^{yy}}\right)$$

$$K_{v\theta} = -\cos\Phi \; K_{\alpha\beta},$$

$$K_{vp} = M_{\alpha\mu}{}^y,$$

$$K_{\theta u} = K_{\alpha\beta\gamma^x} \theta\gamma,$$

$$K_{\theta v} = K_{\alpha\beta\gamma^y} \theta\gamma$$

$$K_{\theta\theta} = K_{\alpha\beta\gamma'} U_\beta + K_{\alpha\beta\gamma'} V_\beta + \frac{1}{\Pr\sqrt{Gr}}\left(S_{\alpha\beta^{xx}} + S_{\alpha\beta^{yy}}\right)$$
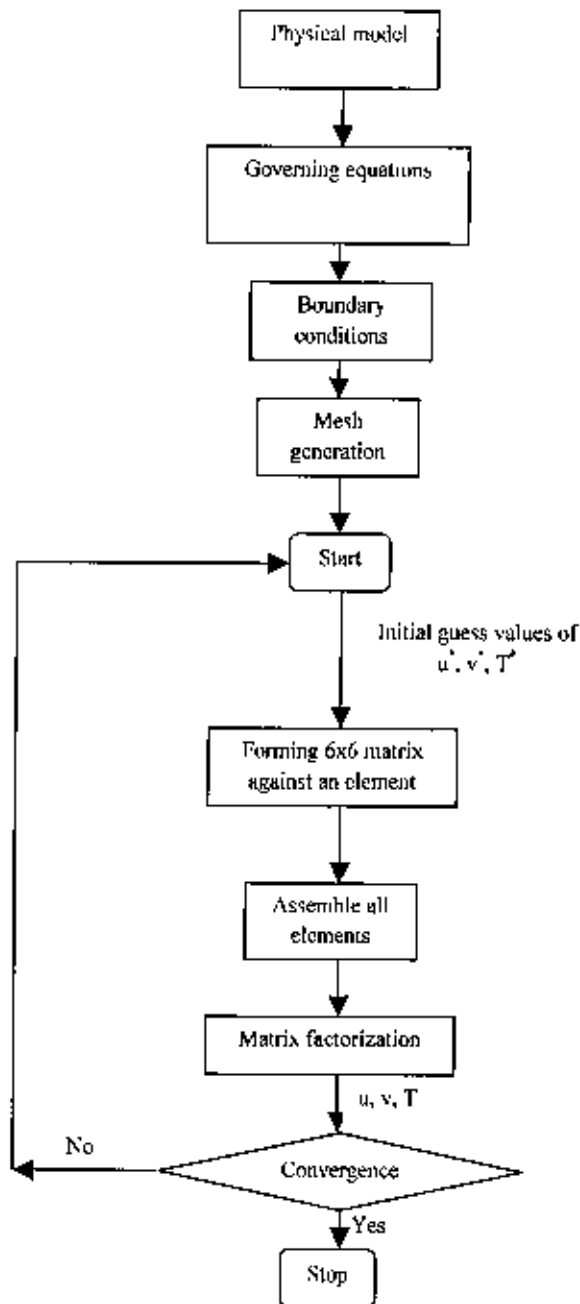
$$K_{\theta p} = 0, \; K_{pu} = K_{\alpha\beta}{}^x, \; K_{pv} = K_{\alpha\beta}{}^y \; \text{and} \; K_{p\theta} = 0 = K_{pp}.$$

The iteration process is terminated if the percentage of the overall change compared to the previous iteration is less than the specified value.

To solve the sets of the global nonlinear algebraic equations in the form of matrix, the Newton-Raphson iteration technique has been adapted through PDE solver with MATLAB interface.

3.6.1 ALGORITHM

In the iterative Newton-Raphson algorithm, the discrete forms of the continuity, momentum and energy equations are solved to find out the value of the velocity and the temperature. It is essential to guess the initial values of the variables. Then the numerical solutions of the variables are obtained while the convergent criterion is fulfilled.

```
              ┌──────────────────┐
              │  Physical model  │
              └──────────────────┘
                       │
                       ▼
              ┌──────────────────┐
              │ Governing equations │
              └──────────────────┘
                       │
                       ▼
              ┌──────────────────┐
              │    Boundary       │
              │   conditions      │
              └──────────────────┘
                       │
                       ▼
              ┌──────────────────┐
              │     Mesh          │
              │   generation      │
              └──────────────────┘
                       │
                       ▼
              ┌──────────────────┐
              │     Start         │
              └──────────────────┘
```

Initial guess values of u^*, v^*, T^*

```
              ┌──────────────────┐
              │ Forming 6x6 matrix │
              │ against an element │
              └──────────────────┘
                       │
                       ▼
              ┌──────────────────┐
              │  Assemble all     │
              │   elements        │
              └──────────────────┘
                       │
                       ▼
              ┌──────────────────┐
              │ Matrix factorization │
              └──────────────────┘
```

u, v, T

No ◄─────── Convergence

Yes

Stop

3.7 SOLUTION OF SYSTEM OF EQUATIONS

A system of linear algebraic equations has been solved by the UMFPACK with MATLAB interface. UMFPACK is a set of routines for solving asymmetric sparse linear systems, $Ax = b$, using the Asymmetric Multi Frontal method and direct sparse LU factorization. Five primary UMFPACK routines are required to factorize A or $Ax = b$:

1. Pre-orders the columns of A to reduce fill-in and performs a symbolic analysis.

2. Numerically scales and then factorizes a sparse matrix.

3. Solves a sparse linear system using the numeric factorization.

4. Frees the Symbolic object.

5. Frees the Numeric object.

Additional routines are:

1. Passing a different column ordering

2. Changing default parameters

3. Manipulating sparse matrices

4. Getting LU factors

5. Solving the LU factors

6. Computing determinant

UMFPACK factorizes PAQ, PRAQ, or $PR^{-1}AQ$ into the product LU, where L and U are lower and upper triangular, respectively, P and Q are permutation matrices, and R is a diagonal matrix of row scaling factors (or $R = I$ if row-scaling is not used). Both P and Q are chosen to reduce fill-in (new non zeros in L and U that are not present in A). The permutation P has the dual role of reducing fill-in and maintaining numerical accuracy (via relaxed partial pivoting and row interchanges). The sparse matrix A can be square or rectangular, singular or non-singular, and real or complex (or any combination). Only square matrices A can be used to solve $Ax = b$ or related systems. Rectangular matrices can only be factorized. UMFPACK first finds a column pre-ordering that reduces fill-in, without regard to numerical values. It scales and analyzes the matrix, and then automatically selects one of three strategies for pre-ordering the rows and columns: asymmetric, 2-by-2, and symmetric. These strategies are described below.

One notable attribute of the UMFPACK is that whenever a matrix is factored, the factorization is stored as a part of the original matrix so that further operations on the matrix can reuse this factorization. Whenever a factorization or decomposition is calculated, it is preserved as a list (element) in the factor slot of the original object. In this way a sequence of operations, such as

determining the condition number of a matrix and then solving a linear system based on the matrix, do not require multiple factorizations of the intermediate results.

Conceptually, the simplest representation of a sparse matrix is as a triplet of an integer vector i giving the row numbers, an integer vector j giving the column numbers, and a numeric vector x giving the non-zero values in the matrix. The triplet representation is row-oriented if elements in the same row were adjacent and column-oriented if elements in the same column were adjacent. The compressed sparse row or compressed sparse column (csc) representation is similar to row-oriented triplet or column-oriented triplet respectively. These compressed representations remove the redundant row or column in indices and provide faster access to a given location in the matrix.

3. 8 GRID INDEPENDENCE TEST

Preliminary results are obtained to inspect the field variables grid independency solutions. Test for the accuracy of grid fineness has been carried out to find out the optimum grid number.
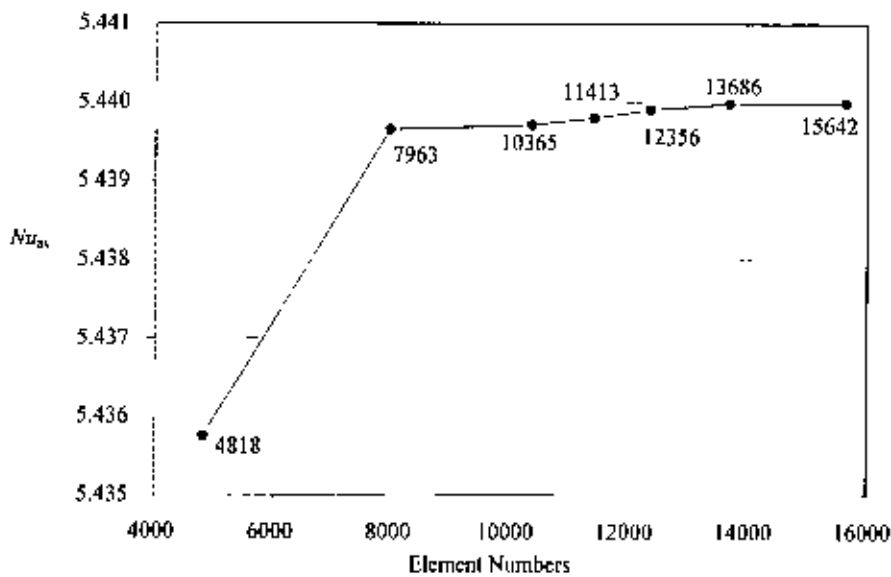
Figure 3.2 Convergence of average Nusselt number with grid refinement for $Gr = 10^6$ and $dr = 0.2$

In order to obtain grid independent solution, a grid refinement study is performed for a rectangular open cavity with $Gr = 10^6$ and $dr = 0.2$. Figure 3.2 shows the convergence of the average Nusselt number, Nu at the heated surface with grid refinement. It is observed that grid independence is achieved with 13686 elements where there is insignificant change in Nu with further increase of mesh elements. Six different non-uniform grids with the following number of nodes and elements were considered for the grid refinement tests: 27342 nodes, 4818 elements;

31

49335 nodes, 7663 elements; 72782 nodes, 10365 elements; 73542 nodes, 11413 elements; 96030 nodes, 12356elements; 982450 nodes, 13686 elements. From these values, 982450 nodes, 13686 elements can be chosen throughout the simulation to optimize the relation between the accuracy required and the computing time.

3.9 MESH GENERATION

In finite element method, the mesh generation is the technique to subdivide a domain into a set of sub-domains, called finite elements. Fig 3.3 shows a domain, Λ is subdivided into a set of sub-domains, Λ^e with boundary Γ^e.
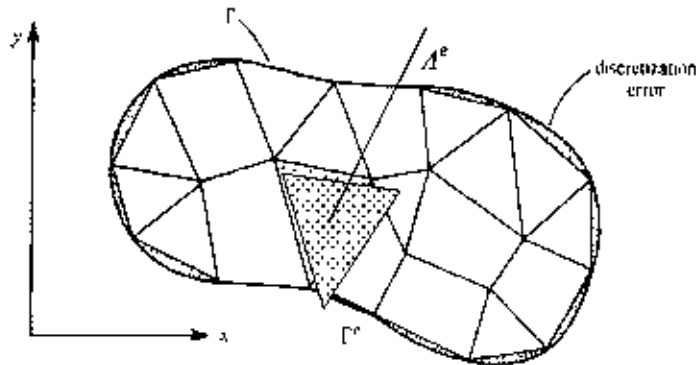
Figure 3.3: Finite element discretization of a domain

The present numerical technique will discretize the computational domain into unstructured triangles by Delaunay Triangular method. The Delaunay triangulation is a geometric structure that has enjoyed great popularity in mesh generation since the mesh generation was in its infancy. In two dimensions, the Delaunay triangulation of a vertex set maximizes the minimum angle among all possible triangulations of that vertex set.

Figure 3.4 shows the mesh mode for the present numerical computation. Mesh generation has been done meticulously.
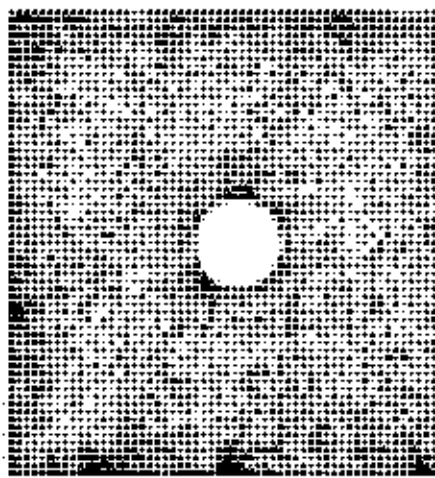
Figure 3.4: Current mesh structure of elements for rectangular open cavity.

RESULTS AND DISCUSSION

Two-dimensional laminar steady state natural convection flow in a rectangular open cavity with the left vertical wall is at constant heat flux has been studied numerically, as shown in Figure 3.1. An adiabatic circular cylinder is placed at the center of the cavity and the opposite wall to the aperture is heated by a constant heat flux. The top and bottom walls are kept at the constant temperature. Two-dimensional forms of Navier-Stokes equations along with the energy equations are solved using Galerkin finite element method. Results are obtained for a range of Grashof number from 10^3 to 10^6 at Pr = 0.72, 1.0 and 7.0 with constant physical properties. The parametric studies for a wide range of governing parameters show consistent performance of the present numerical approach to obtain as stream functions and temperature profiles. The computational results indicate that the heat transfer coefficient is strongly affected by Grashof number. Using Nusselt number and Grashof number develops an empirical correlation. Obviously for high values of Grashof number the errors encountered are appreciable and hence it is necessary to perform some grid size testing in order to establish a suitable grid size. Grid independent solution is ensured by comparing the results of different grid meshes for Gr = 10^6, which was the highest Grashof number. The total domain is discretized into 4806 elements that result in 32643 nodes.

The effect of inclination angle is examined for $\Phi = 0°, 10°, 30°, 45°$ with aspect ratio A = 1. A comparison between the steady-state patterns of streamlines from Grashof numbers of 10^3 to 10^6 with different angles is presented in Figure 4.1 – 4.15. Also a comparison between the steady-state patterns of isotherms from Grashof numbers of 10^3 to 10^6 with different angles is presented in Figure 4.1 – 4.15. For the isotherm, the figures show that as the Grashof number and the inclination angle increases, the buoyancy force increases and the thermal boundary layers become thinner. For the streamlines, the figures show that the fluid enters from the bottom of the aperture, circulates in a clockwise direction following the shape of the cavity, and leaves toward the upper part of the aperture. The streamline patterns is very similar for first one Grashof number and the inclination angle, but the fluid moves faster for Gr = 10^4. Also, for Gr = 10^5 and 10^6, the streamline patterns is similar but the upper boundary layer becomes thinner and faster, the velocity of the air flow moving toward the aperture increases, and the area that is occupied by the leaving hot fluid decreases compared with that of the entering fluid. Isotherms and streamlines show that as the inclination angle of the heated wall increases, the velocity gradient increases at upper heated wall, the strength of the circulation increases. The results are presented in terms of streamlines and isotherm patterns. The variations of the average Nusselt number and average temperature are also highlighted. . The results in the steady state are obtained for a

Grashof range from 10^3 to 10^6 and for a range of $0°-45°$ for the inclination angles of the cavity. The results show that for high Grashof numbers, the Nusselt number changes substantially with the inclination angle of the cavity. The numerical model predicted Nusselt number oscillations for low angles and high Grashof numbers.

In order to validate the numerical code, pure natural convection with $Pr = 0.72$ in a square open cavity was solved, and the results were compared with those reported by Hinojosa et al. (2005), obtained with an extended computational domain. In Table 4.1, a comparison between the average Nusselt number is presented. The results from the present experiment are almost same as Hinojosa et al.

Table 4.1: Comparison of the results for the constant surface temperature with $Pr = 0.72$.

Gr	Nu_{av}	
	Present work	Hinojosa et al. (2005)
10^3	1.32	1.30
10^4	3.45	3.44
10^5	7.41	7.44
10^6	14.44	14.51

4.1 EFFECTS OF INCLINATION ANGLE

With the increase of the Grashof number, complex flow pattern characteristics were found for some inclination angles. To show this, the profiles of isotherm and streamline and inclination angles of $0°$, $15°$, $30°$ and $45°$ are presented in Fig. 4.1 to 4.15. For inclination angles of the cavity between $0°$ and $45°$, the steady state can not be reached; the instantaneous pictures show that the fluid enters and leaves in a very irregular way, indicating an unsteady convection. The cold fluid enters by the lower section of the aperture plane, without symmetry, and the hot fluid leaves by the upper section. The velocity magnitude of the leaving fluid is greater than the incoming fluid, and thus the thermal boundary layer at the top wall becomes much thinner. For the tilted angle of $45°$, the air flow entering and leaving the cavity decreases its velocity considerably.

In Table 4.2, average Nusselt number for different cavity's inclination angles and Grashof numbers, obtained with the present model for $Pr = 0.72$ and $dr=0.2$ is presented. Table 4.2 presents the average Nusselt numbers for four Grashof numbers (10^3, 10^4, 10^5 and 10^6) for a range of $0°- 45°$ for the tilted angles of the open cavity. For different angles and Gr numbers, mainly for

lower angles and for higher Gr, the average Nusselt number increases. Therefore, in Table 4.2, the average Nusselt numbers and their standard deviation are reported.

In Fig.4.16, we observe that the heat transfer rate Nu increases with the increase of inclination angles and increase of Grashof number.

Table 4.2: Average Nusselt number Nu for different cavity's inclination angles Φ and Grasof numbers for Pr =0.72 and dr=0.2.

Φ	Nu_{av}			
	Gr=10^3	Gr=10^4	Gr=10^5	Gr=10^6
0°	3.2421358	3.2695525	4.0484195	5.453783
15°	3.244177	3.2988331	4.1695323	5.582469
30°	3.2482889	3.3173974	4.2411466	5.608271
45°	3.2544684	3.3222377	4.271296	5.563731

4.2 EFFECTS OF PRANDTL NUMBER

For investigating the effects of Prandtl number on the flow and heat transfer characteristics, a study for Pr= 0.72, 1.0 and 7.0. The predicted isotherms and stream lines are shown in figure 4.1 to 4.15. It is seen that fluid moves clock wise around the cylinder.

In Table 4.3, average Nusselt numbers for different Prandtl numbers while Pr = 0.72, 1.0 and 7.0 and Grasof numbers, obtained with the present model for angle Φ= 0° and diameter ratio dr = 0.2 is presented.

Figure 4.19 shows the averageNusselt number variation for different Prandtl numbers while Pr= 0.72, 1.0, 7.0 In Fig.4.19, we observe that average Nusselt number Nu decreases with increasing of Grashof number Gr and increasing of Prandtl number Pr. The similar behavior is observed in Fig 4.20, 4.21 and 4.22. Heat transfer characteristics become low for lower Prandtl number Pr = 0.72 and high for higher Pr = 7.0. So the results show insignificant for different angles.

The temperature is higher in the case of Pr = 7.0 than in the case of Pr = 0.72. This is because, the fluid with Pr = 7.0 has a lower thermal diffusivity than that of the fluid with Pr = 0.72. Hence, the fluid with Pr = 7.0 will tend to exchange less heat with surrounding fluid by diffusion.

Table 4.3: Average Nusselt numbers for different Prandtl number while $Pr = 0.72$, 1.0 and 7.0, angle $\Phi = 0°$ and $dr = 0.2$.

Nu_{av}				
Pr	$Gr=10^3$	$Gr=10^4$	$Gr=10^5$	$Gr=10^6$
0.72	3.2421358	3.2695525	4.0484195	5.453783
1.0	3.2313557	3.3345096	4.2389865	5.8061547
7.0	3.2676048	4.1116834	5.7404647	8.434301

4.3 EFFECTS OF DIAMETR RATIO

In Table 4.3, average Nusselt numbers for different diameter ratios while $dr = 0. 2, 0.3$ and 0.4 and Grashof numbers, obtained with the present model for angle $\Phi = 0°$ and Prandlt number $=0.72$ is presented. Figure 4.23 shows average Nusselt number increases with increasing of diameter ratio of the cylinder.

Table 4.4: Average Nusselt numbers for different diameter ratios while $dr = 0. 2, 0.3$ and 0.4, angle $\Phi = 0°$ and $Pr= 0.72$.

Nu_{av}				
dr	$Gr=10^3$	$Gr=10^4$	$Gr=10^5$	$Gr=10^6$
0. 2	3.2421358	3.2695525	4.0484195	5.453783
0.3	3.188554	3.2096665	4.0131702	5.459415
0.4	3.1257522	3.1240125	3.9524283	5.453659

CONCLUSION

Two-dimensional laminar steady state natural convection flow in a rectangular open cavity with the left vertical wall is at constant heat flux has been studied numerically. A finite element method for steady-state incompressible natural convection flow is presented. The finite element equations were derived from the governing flow equations that consist of the conservation of mass, momentum, and energy equations. The derived finite element equations are nonlinear requiring an iterative technique solver. The Newton-Raphson iteration method has applied to solve these nonlinear equations for solutions of the nodal velocity component, temperature. and pressure by considering Prandtl numbers between 0.72, 1.0 and 7.0 and Grashof numbers between 10^3 to 10^6. The results show that

❖ Heat transfer depends on Prandtl number and heat transfer rate increases for higher Prandtl number.

❖ Thermal boundary layer thickness is thinner for increasing of Grashof nummber.

❖ The heat transfer rate decreases for certain Grashof number (10^3) and increases gradually for increasing of Grashof number.

❖ The heat transfer rate Nu increases with the increase of inclination angles and increase of Grashof number.

❖ The heat transfer rate Nu increases with the increase of diameter ratio and increase of Grashof number.

❖ Various vortices entering into the flow field and a secondary vortex at the center of the cavity is seen in the streamlines.

EXTENSION OF THIS WORK

In this work, we considered two-dimensional laminar steady-state natural convection in a rectangular open cavity. An adiabatic circular cylinder is placed at the center of the cavity and the left sidewall is heated by a constant heat flux. The top and bottom walls are kept at the ambient constant temperature.

❖ If we consider the heated cylinder inside the cavity instead of adiabatic cylinder then we can extend our problem.

❖ Also taking the non-uniform surface temperature, the problem can be extended.
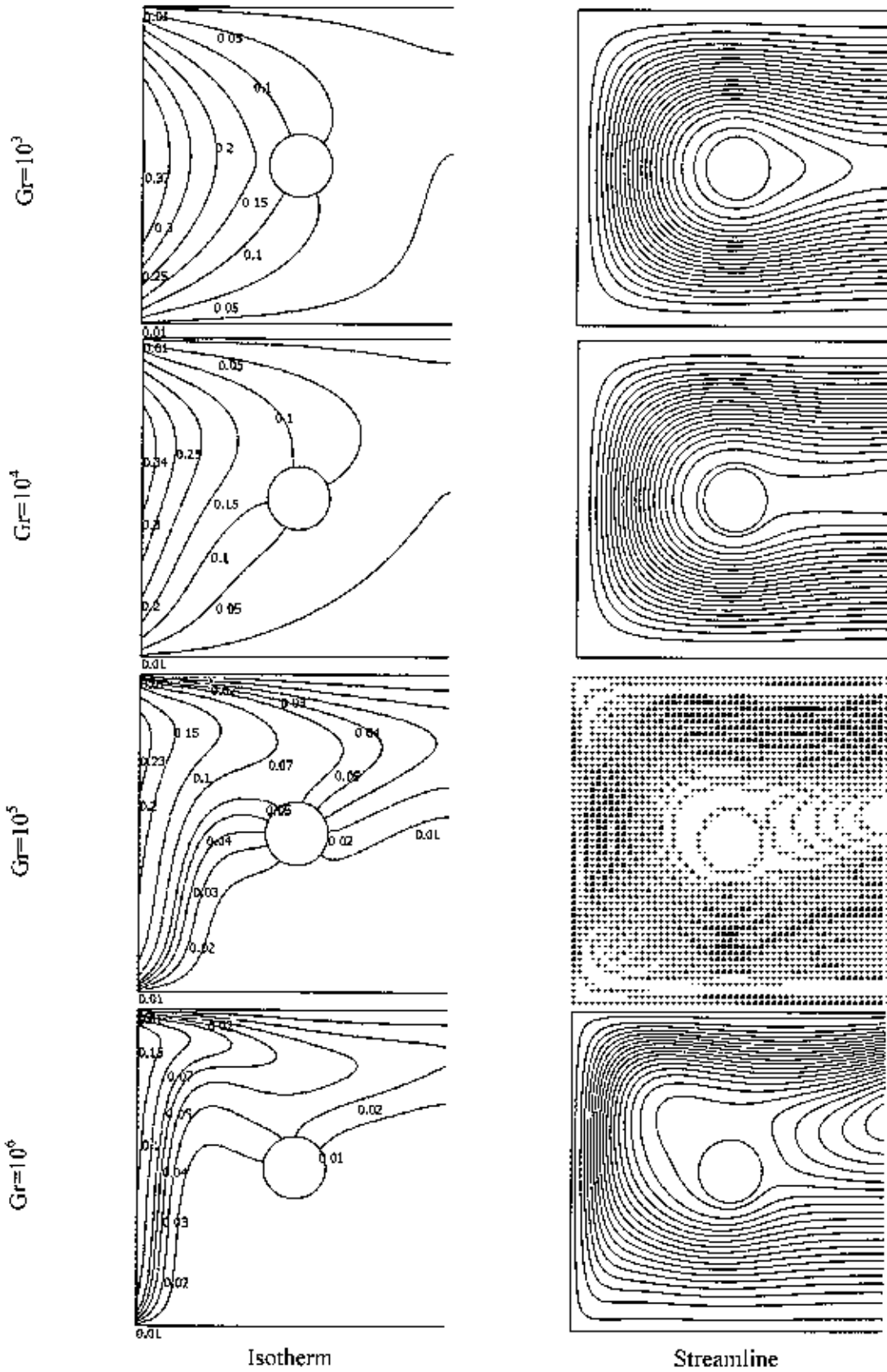
Fig4.1: Isotherms and streamlines patterns for $dr = 0.2$ and $Pr = 0.72$ at angle $0°$

Isotherm   Streamline
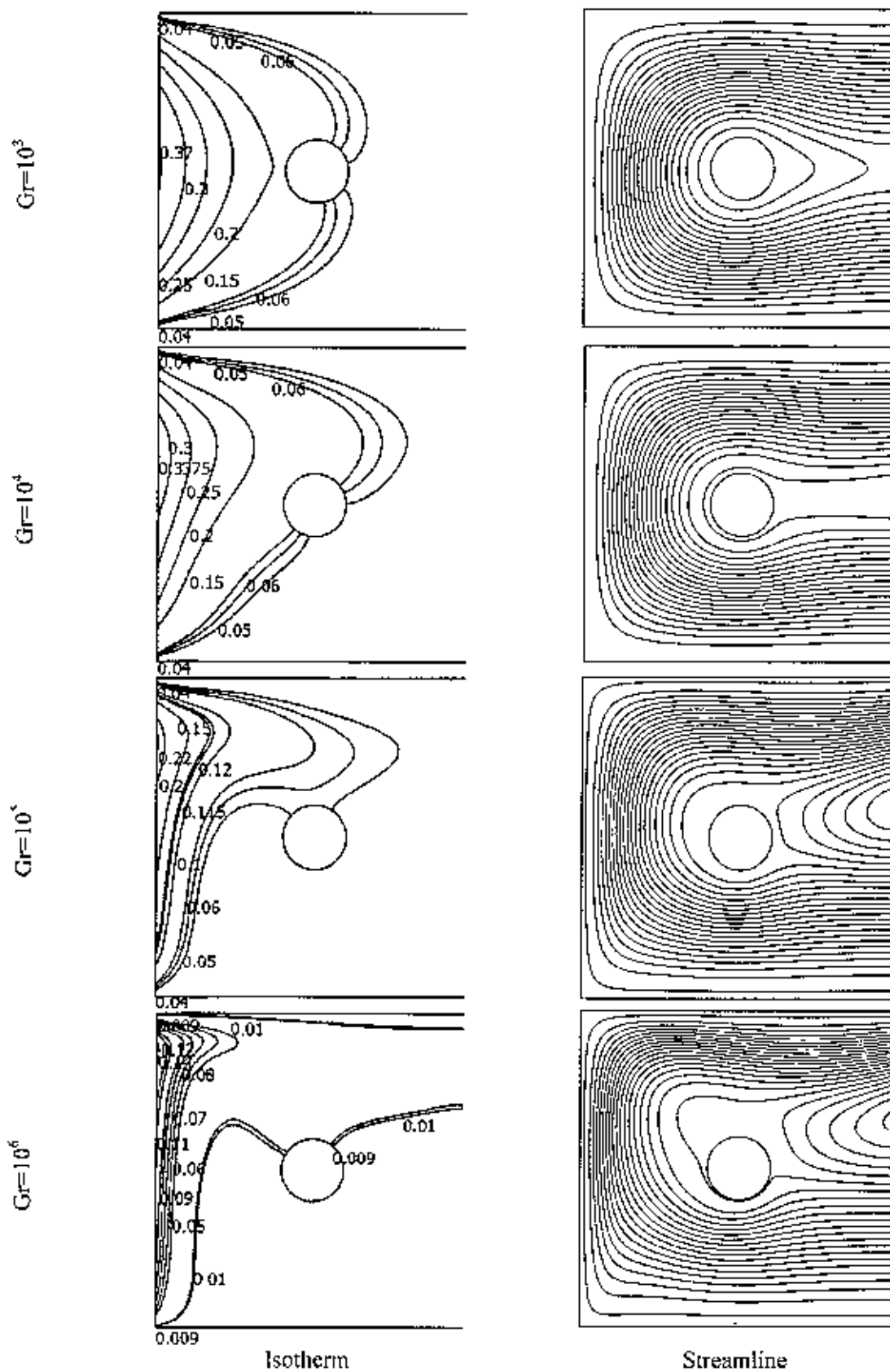
Fig 4.2: Isotherms and streamlines patterns for $dr = 0.2$ and $Pr = 0.72$ at angle $15°$

40

Isotherm   Streamline

Fig 4.3: Isotherms and streamlines patterns for $dr = 0.2$ and $Pr = 0.72$ at angle 30^0

41
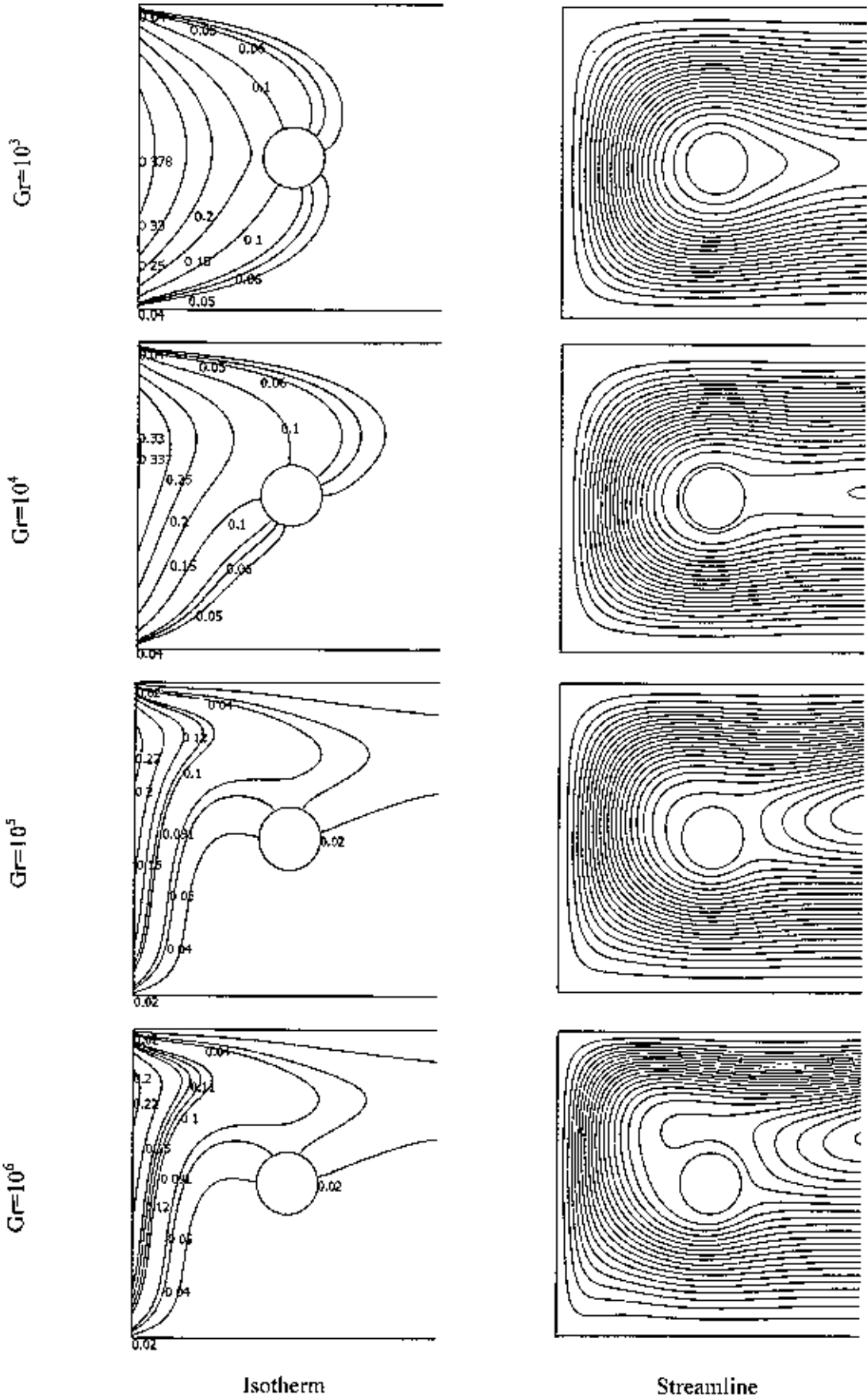
Isotherm   Streamline
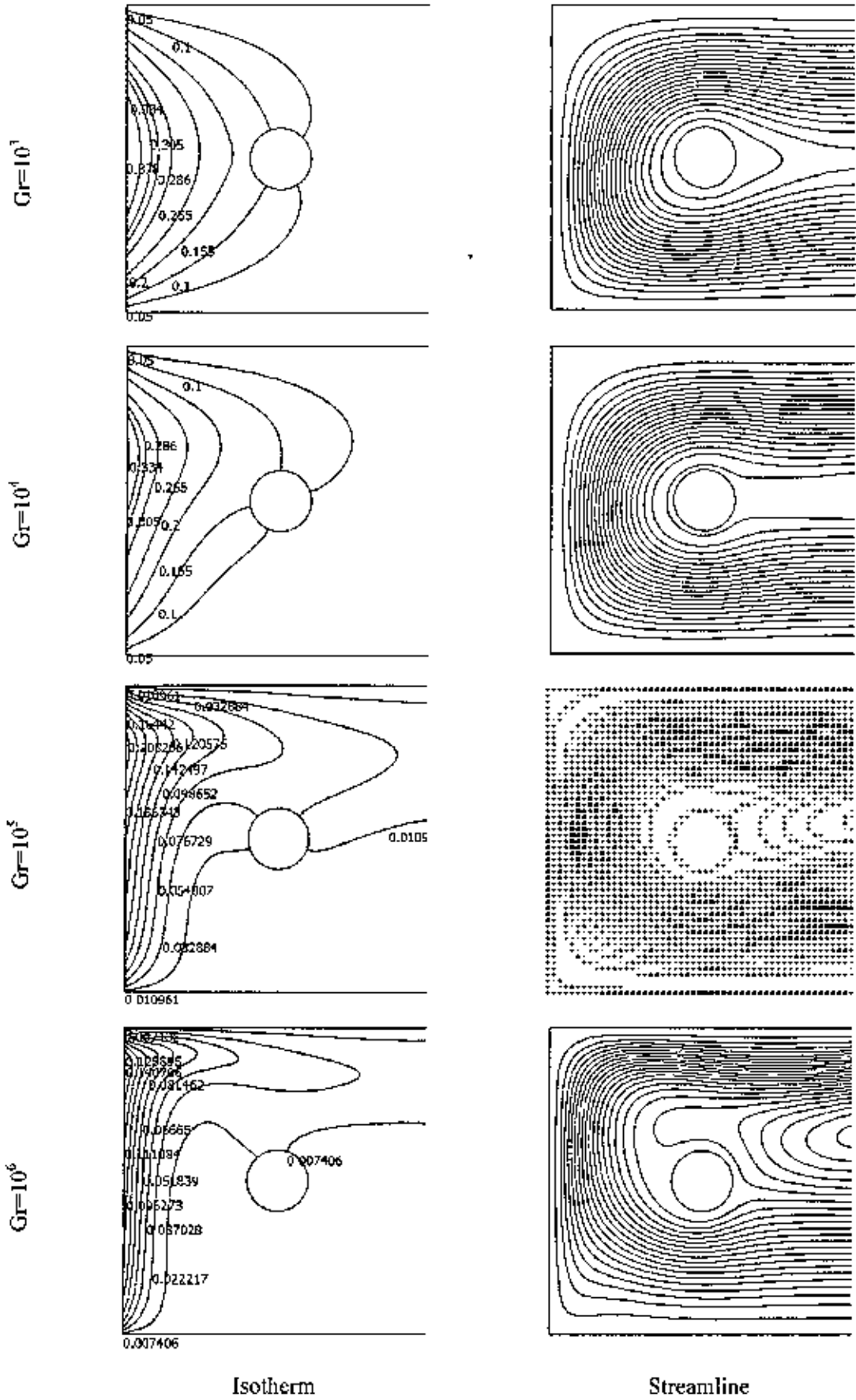
Fig 4.4: Isotherms and streamlines patterns for $dr = 0.2$ and $Pr = 0.72$ at angle 45^0

Isotherm   Streamline
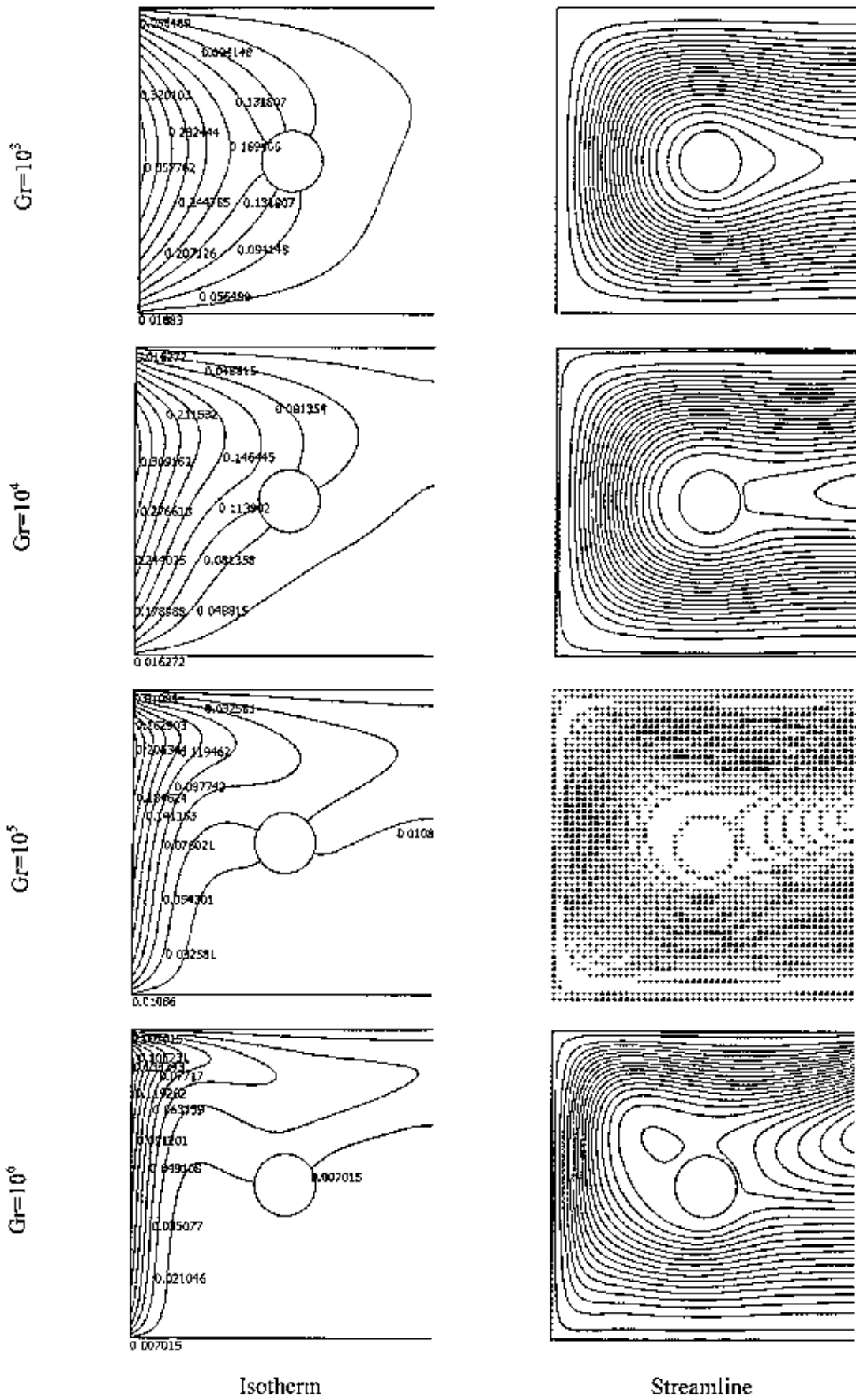
Fig 4.5: Isotherms and streamlines patterns for $dr = 0.2$ and $Pr = 1.0$ at angle $0°$

43

Isotherm   Streamline
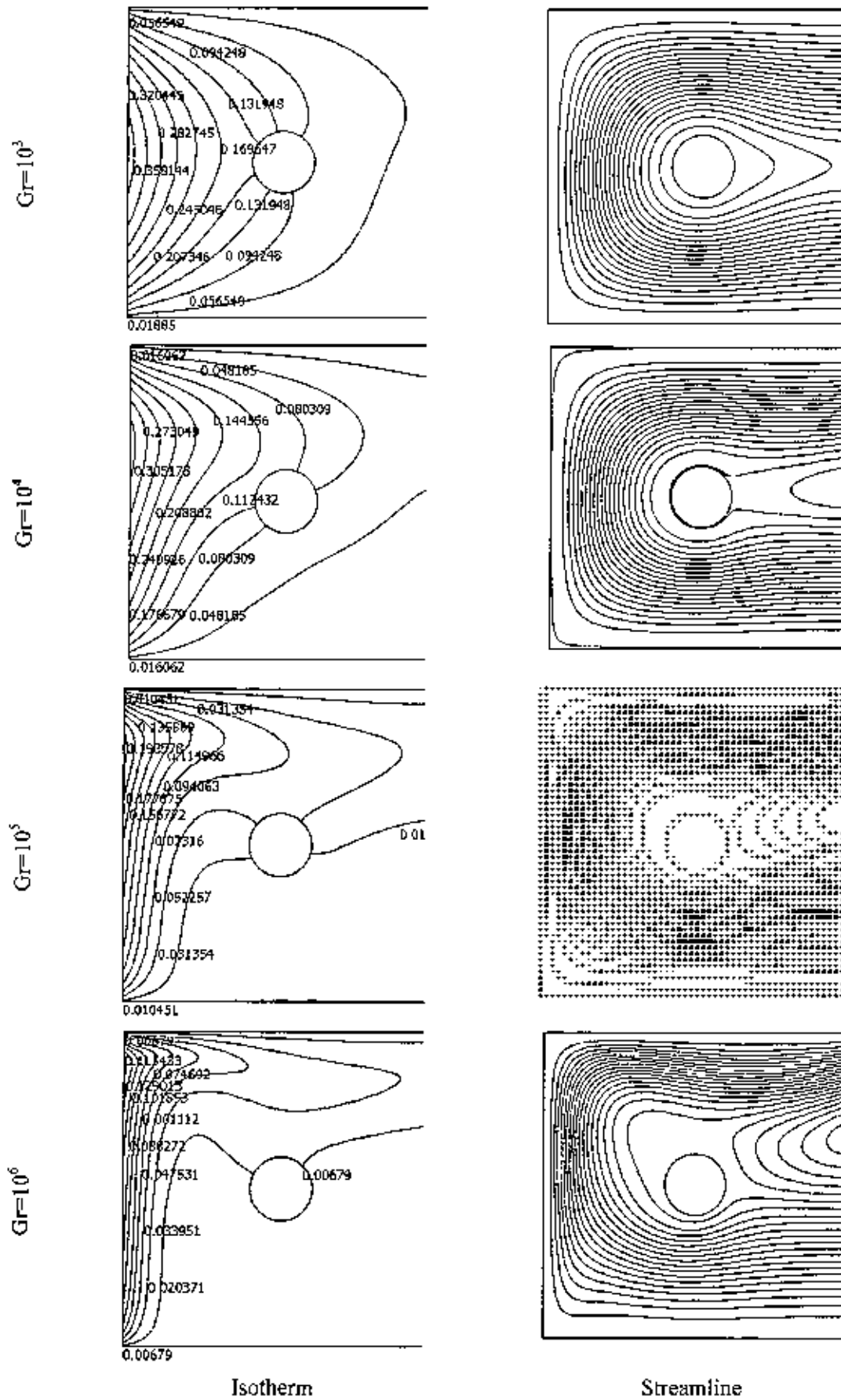
Fig4.6: Isotherms and streamlines patterns for $dr = 0.2$ and $Pr = 1.0$ at angle 15°

44

Isotherm   Streamline
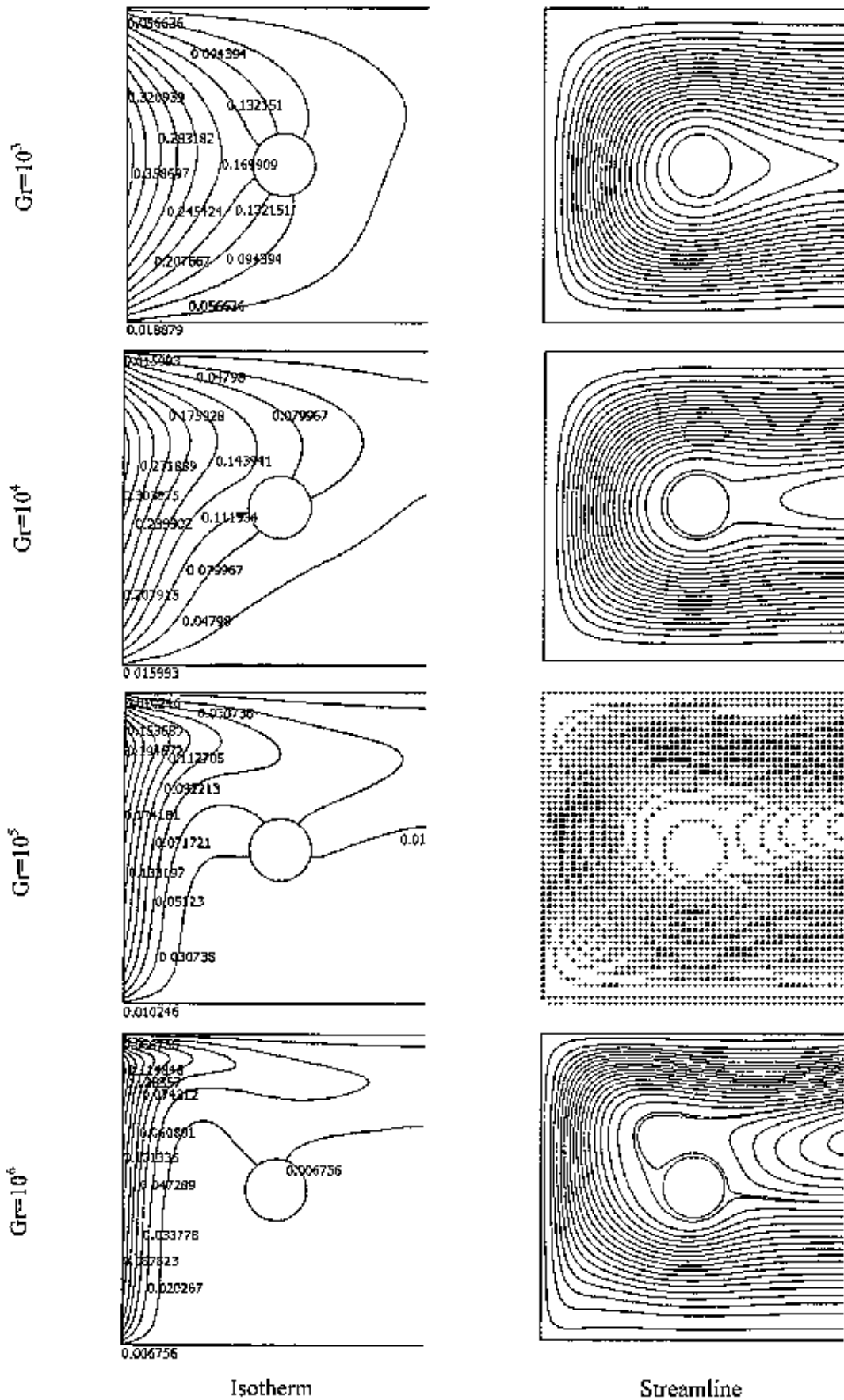
Fig 4.7: Isotherms and streamlines patterns for $dr = 0.2$ and $Pr = 1.0$ at angle $30°$

45

Isotherm   Streamline
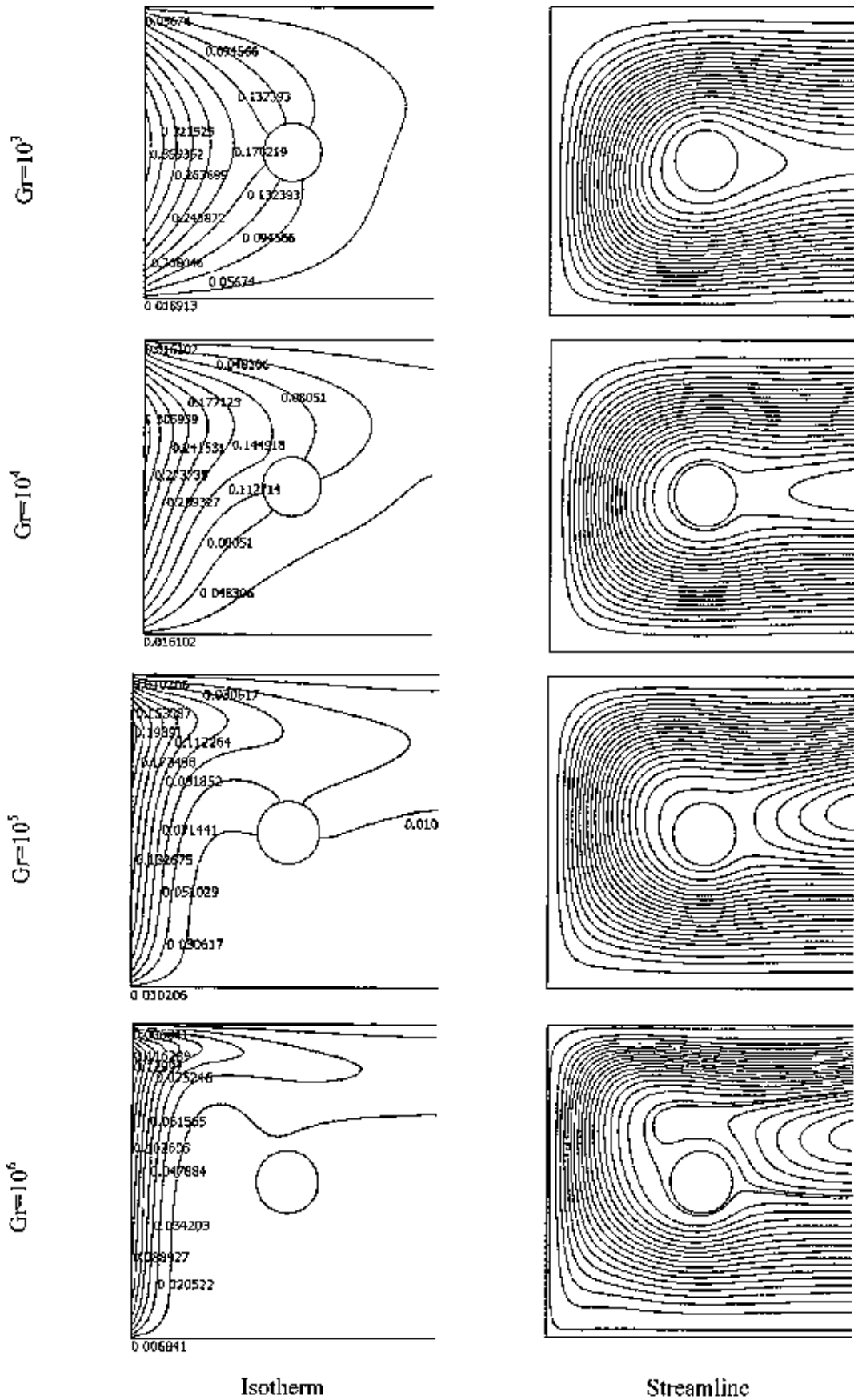
Fig 4.8: Isotherms and streamlines patterns for $dr = 0.2$ and $Pr = 1.0$ at angle $45°$

46

Isotherm   Streamline
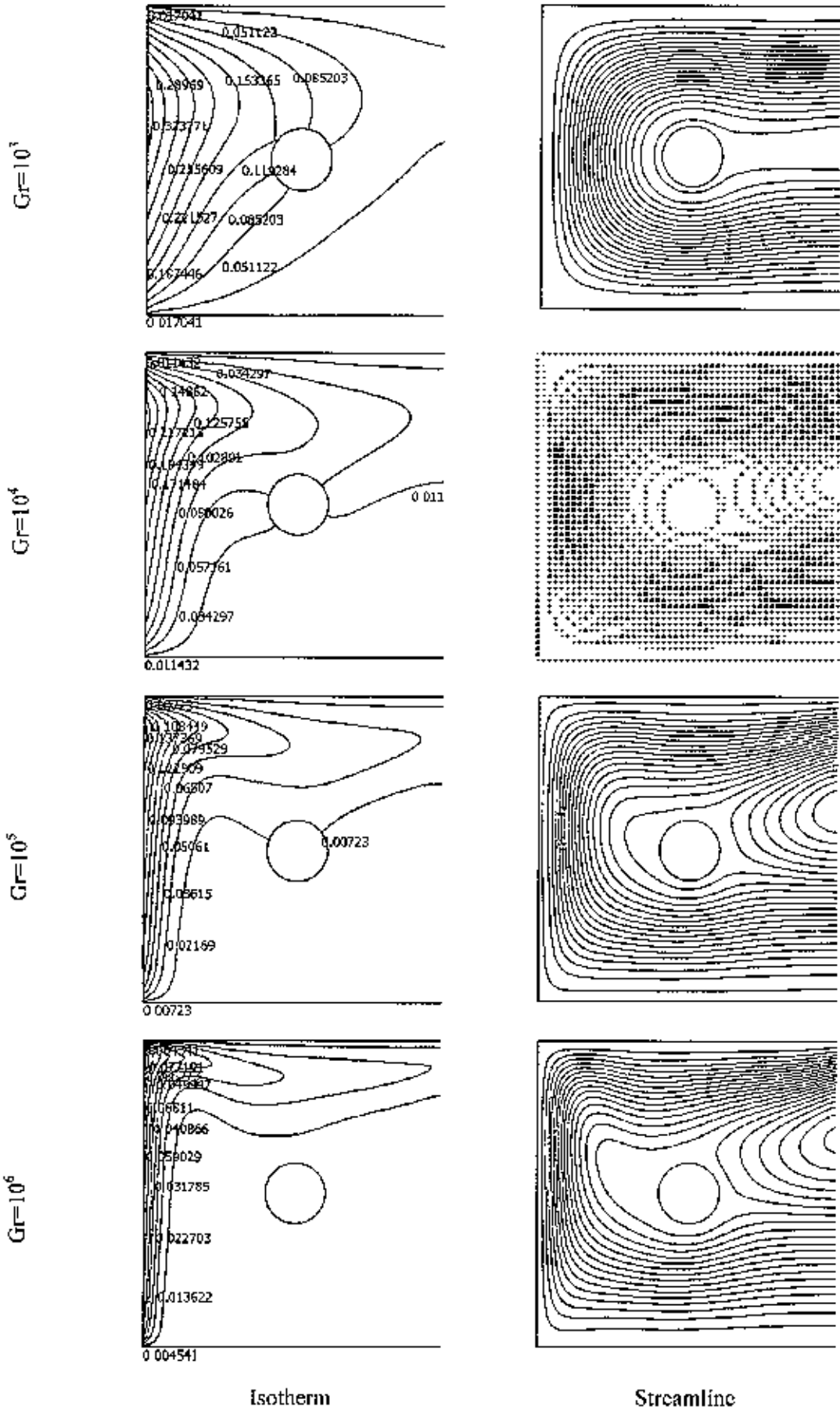
Fig 4 9: Isotherms and streamlines patterns for $dr = 0.2$ and $Pr = 7.0$ at angle 0^0

47

Isotherm   Streamline
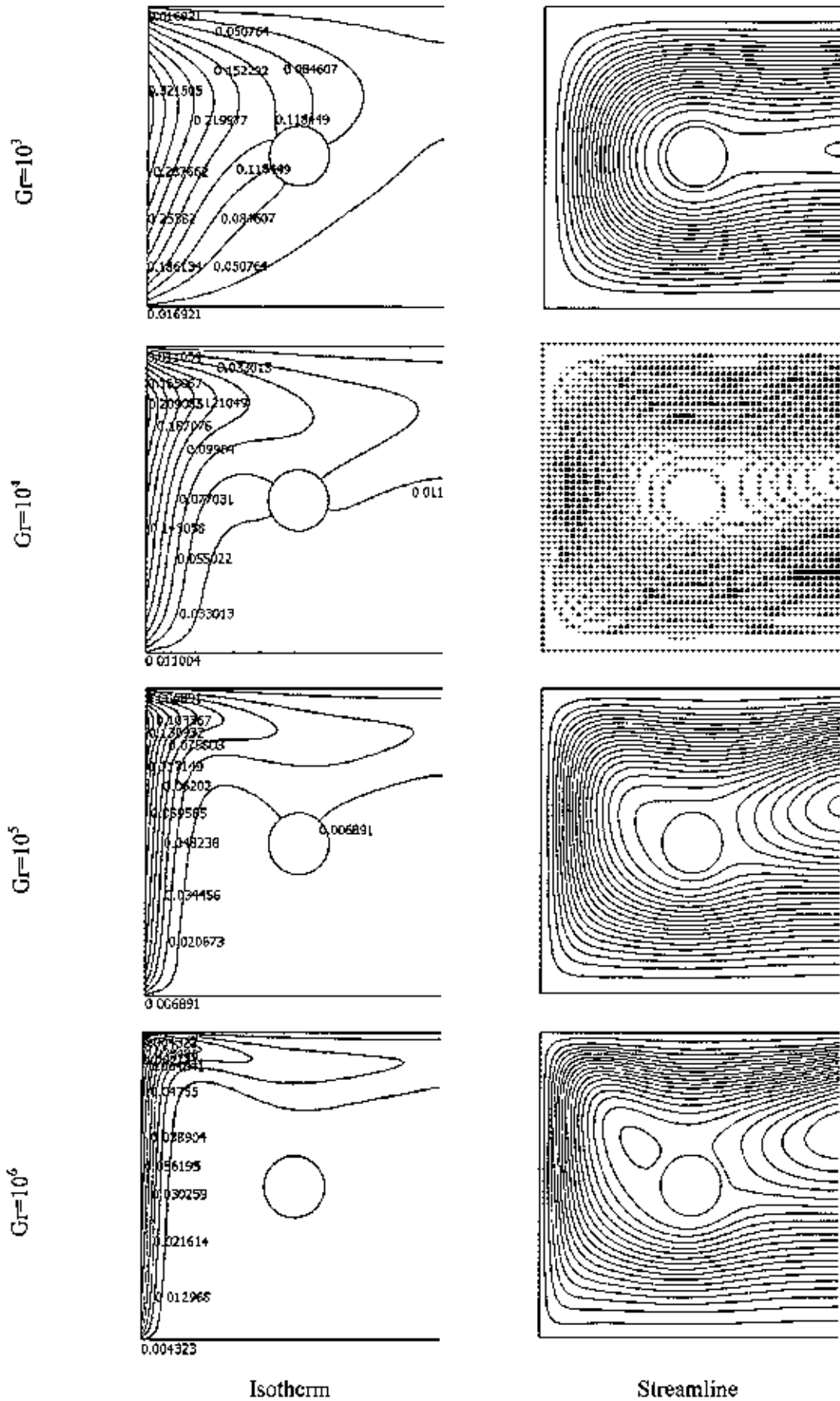
Fig 4.10:Isotherms and streamlines patterns for $dr = 0.2$ and $Pr = 7.0$ at angle $15°$

48

Isotherm   Streamline
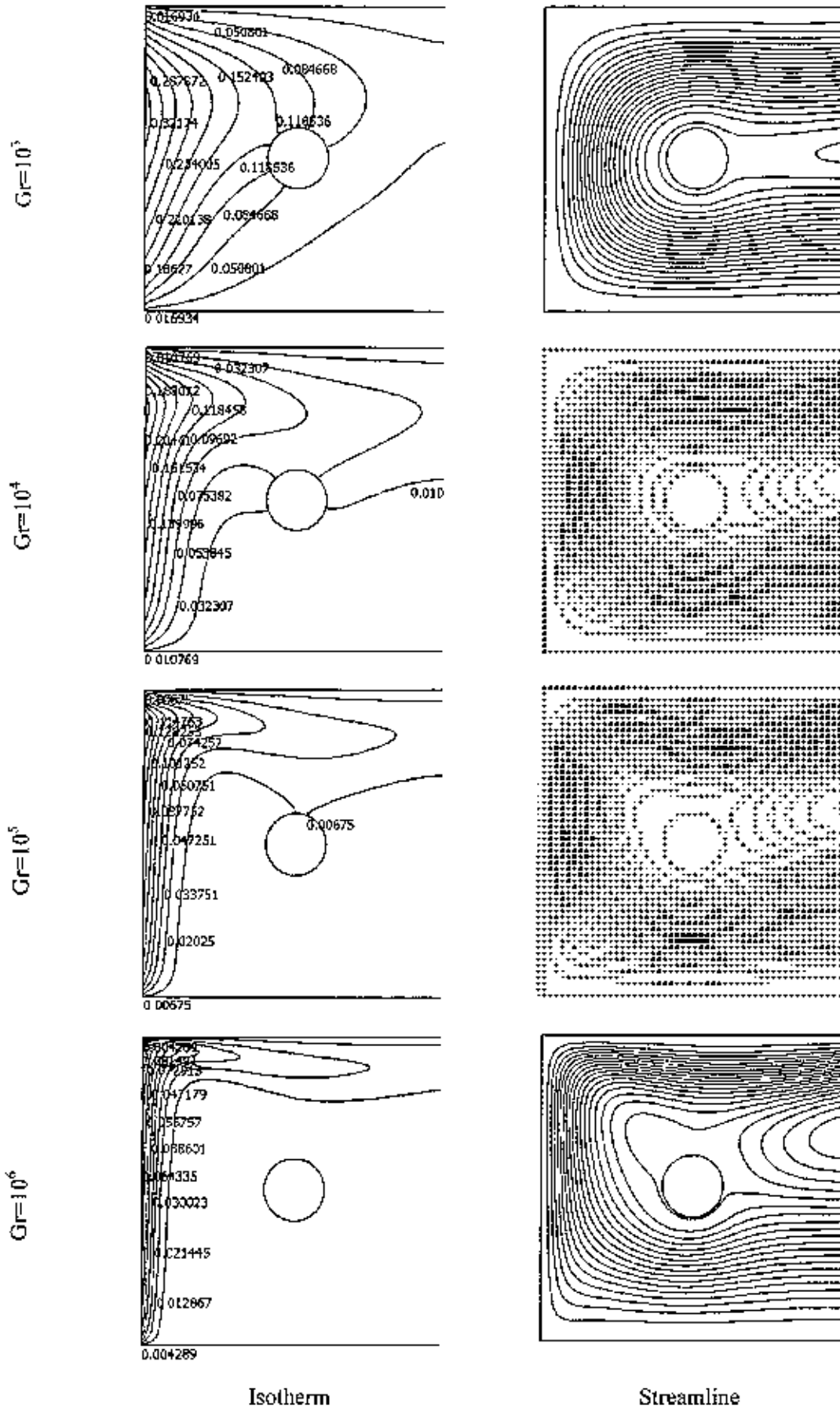
Fig 4.11: Isotherms and streamlines patterns for $dr = 0.2$ and $Pr = 7.0$ at angle $30°$

49

Isotherm   Streamline
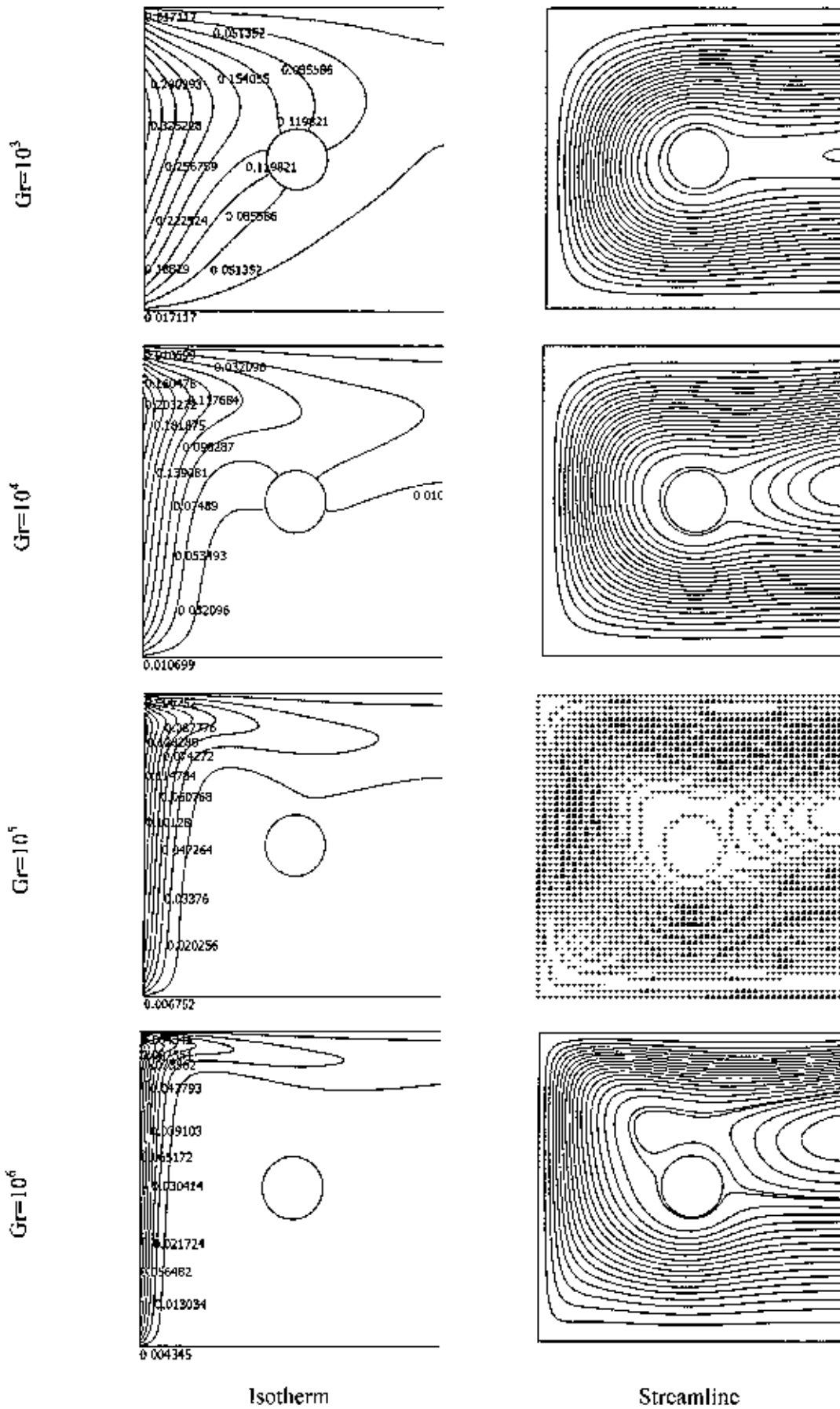
Fig 4.12. Isotherms and streamlines patterns for $dr = 0.2$ and $Pr = 7.0$ at angle $45°$

50

Gr=10³

Gr=10⁴

Gr=10⁵

Gr=10⁶

Isotherm

Streamline

Fig 4.13. Isotherms and streamlines patterns for $dr = 0.3$ and $Pr = 0.72$ at angle $0°$

Gr = 10^3

Gr = 10^4

Gr = 10^5

Gr = 10^6
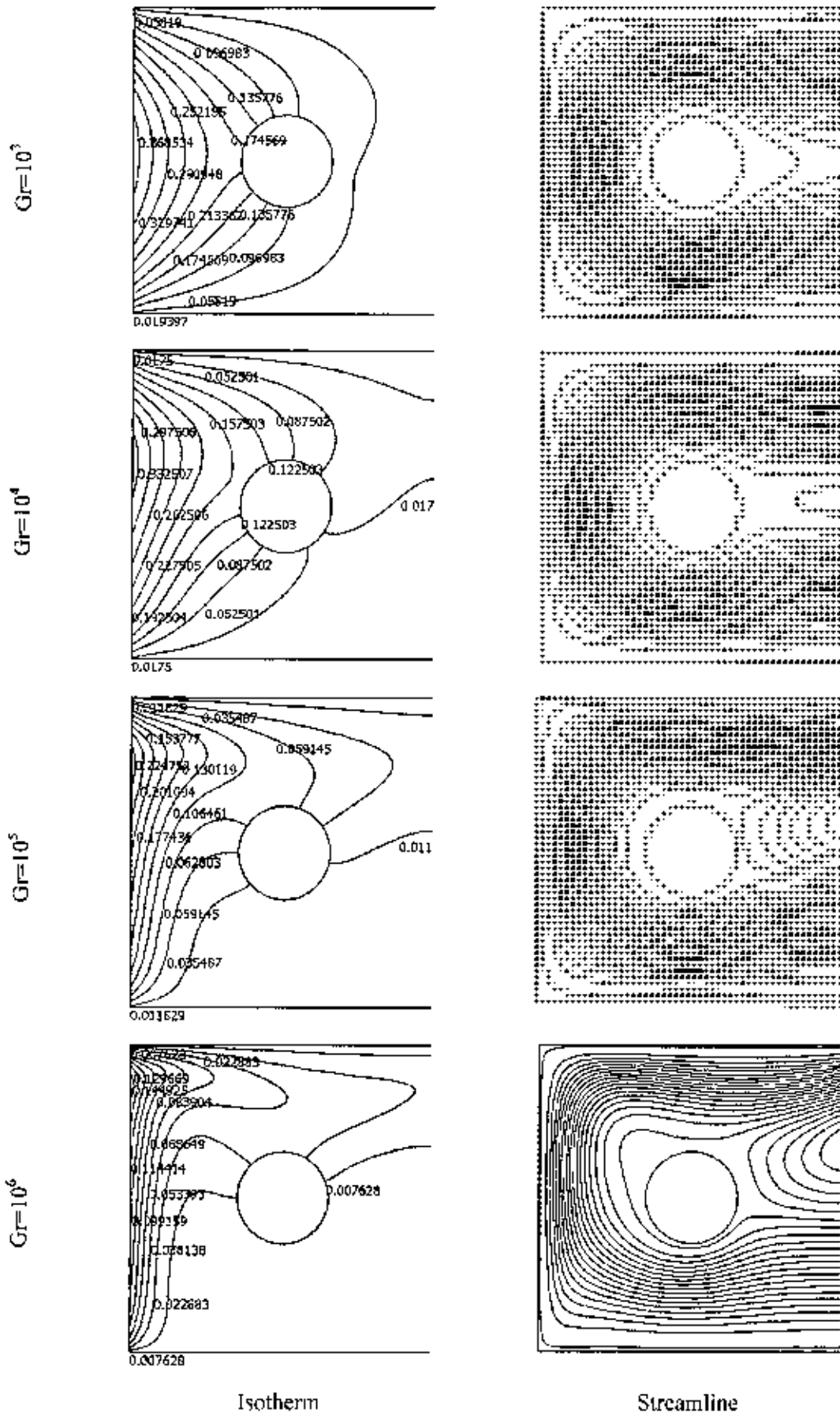
Isotherm
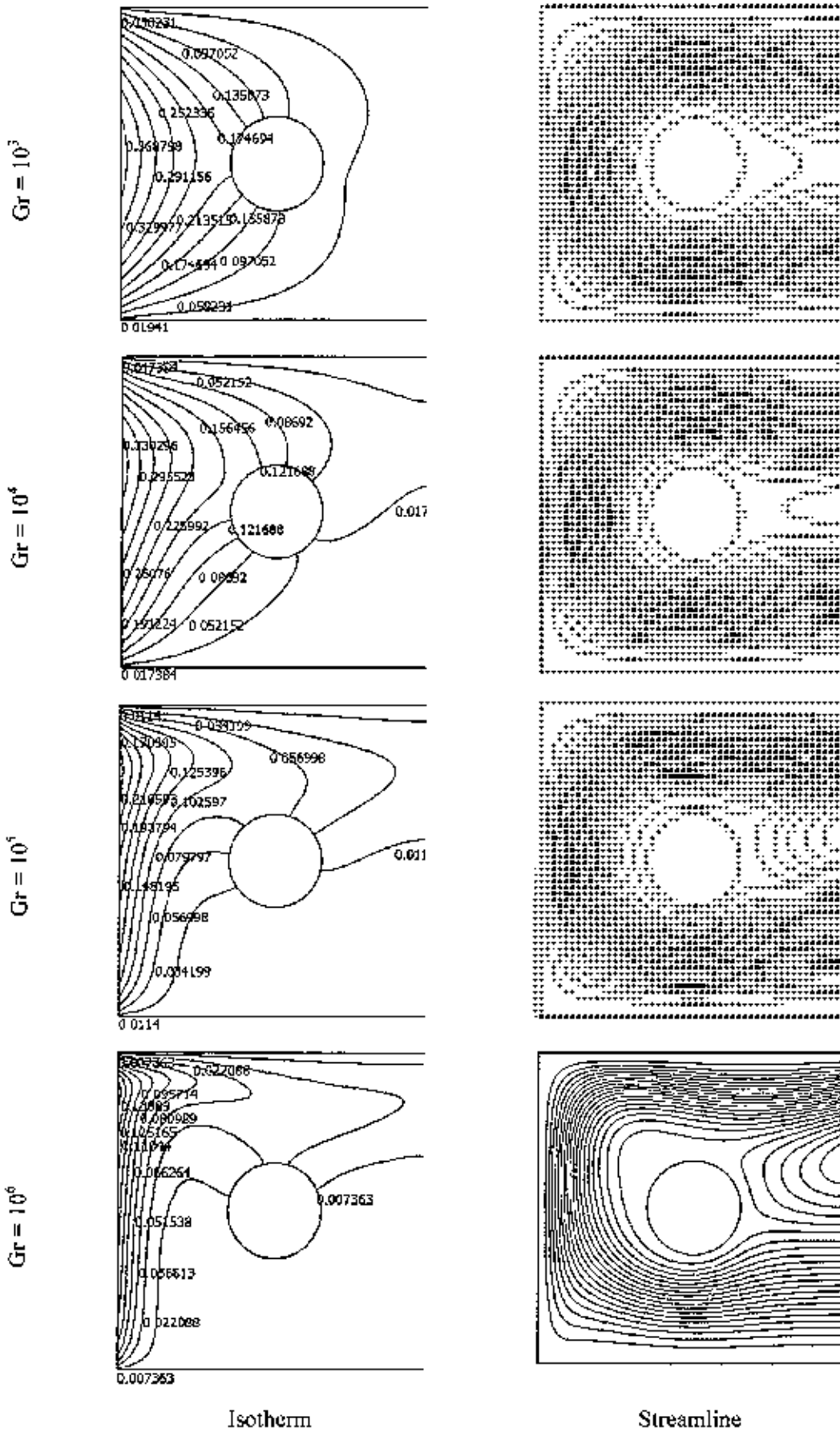
Streamline

Fig 4.14: Isotherms and streamlines patterns for $dr = 0.3$ and $Pr = 0.72$ at angle 15°

Isotherm   Streamline
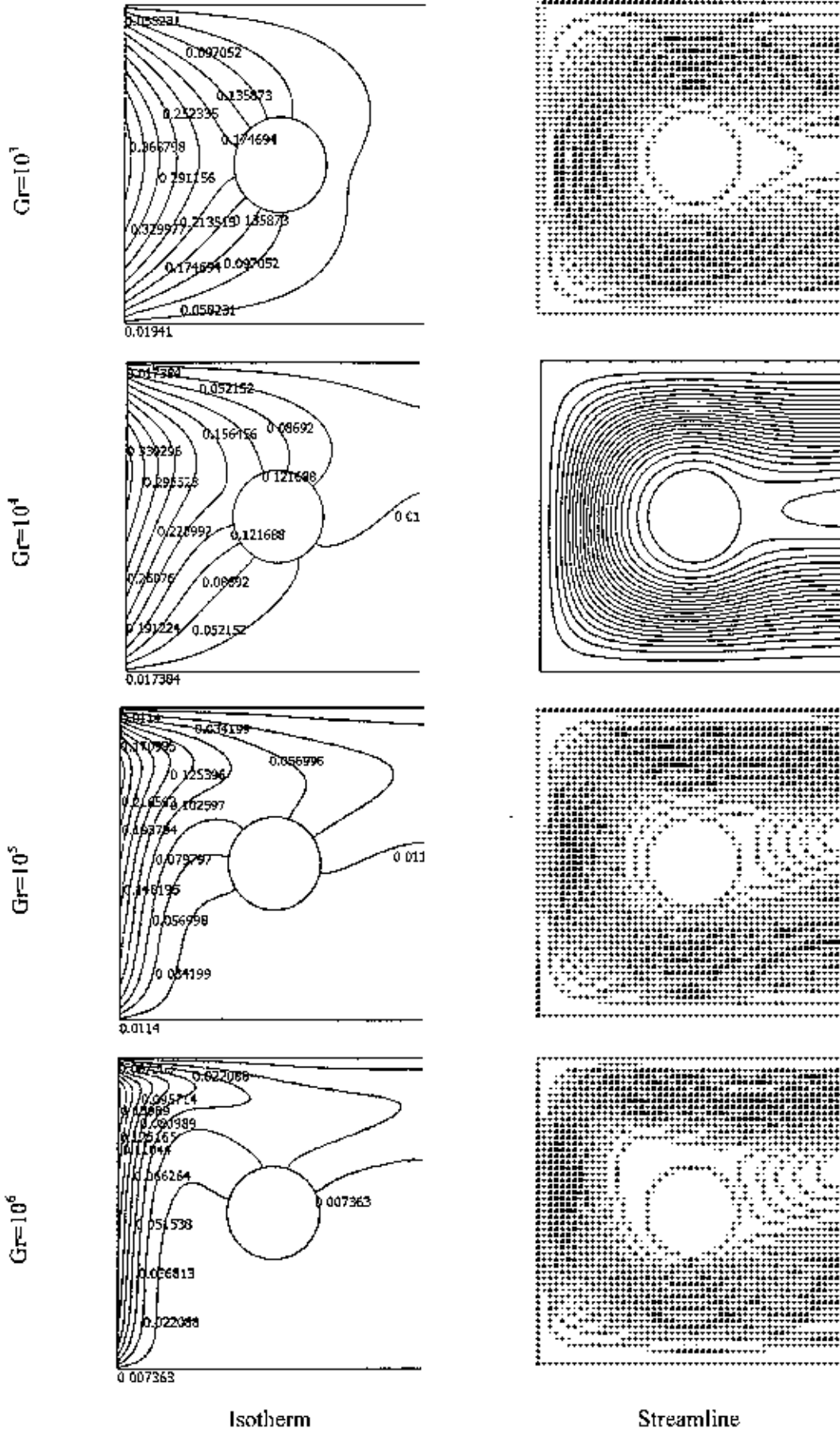
Fig 4.15: Isotherms and streamlines patterns for $dr = 0.3$ and $Pr = 0.72$ at angle $30°$
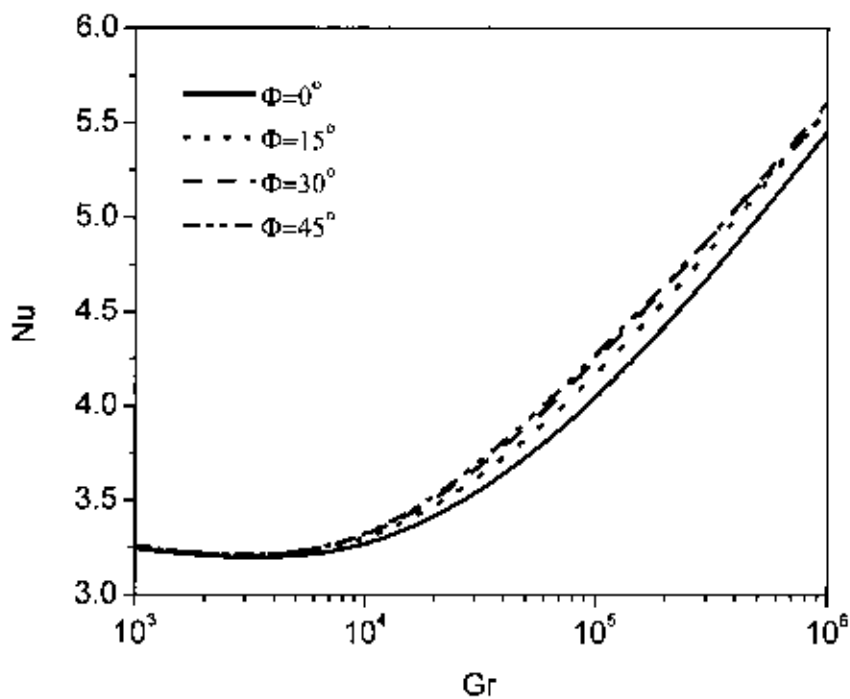
Fig.4.16: Effect of inclination angle on average Nusselt number and Grashof number while $Pr = 0.72$, $dr = 0.2$.
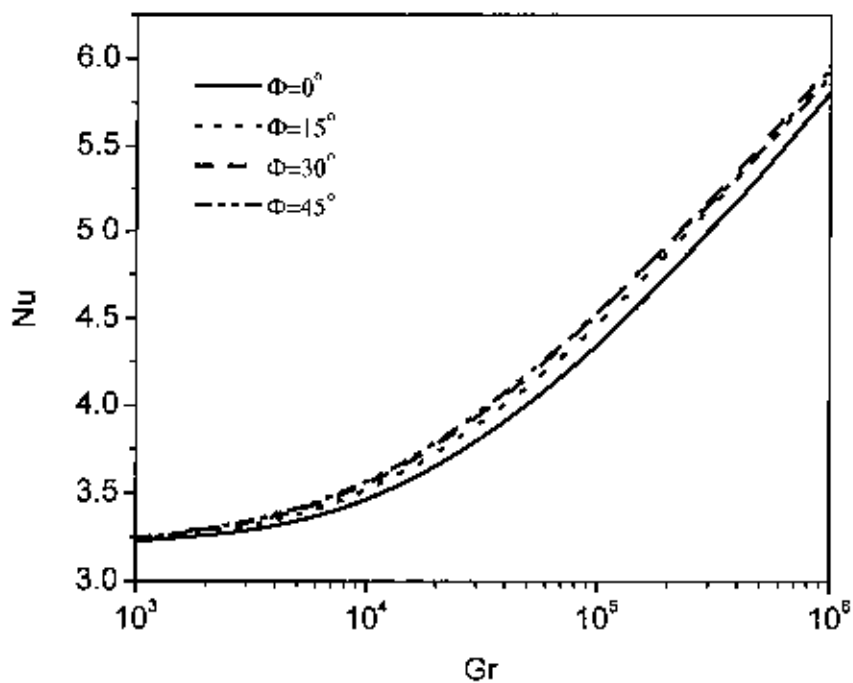
Fig.4.17: Effect of inclination angle on average Nusselt number and Grashof number while $Pr = 1.0$, $dr = 0.2$.
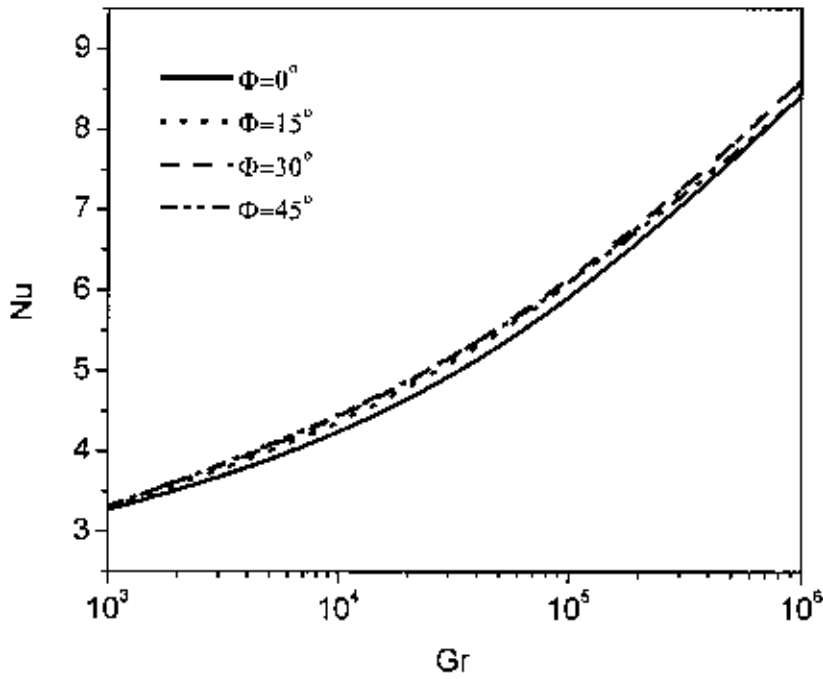
54

Fig.4.18: Effect of inclination angle on average Nusselt number and Grashof number
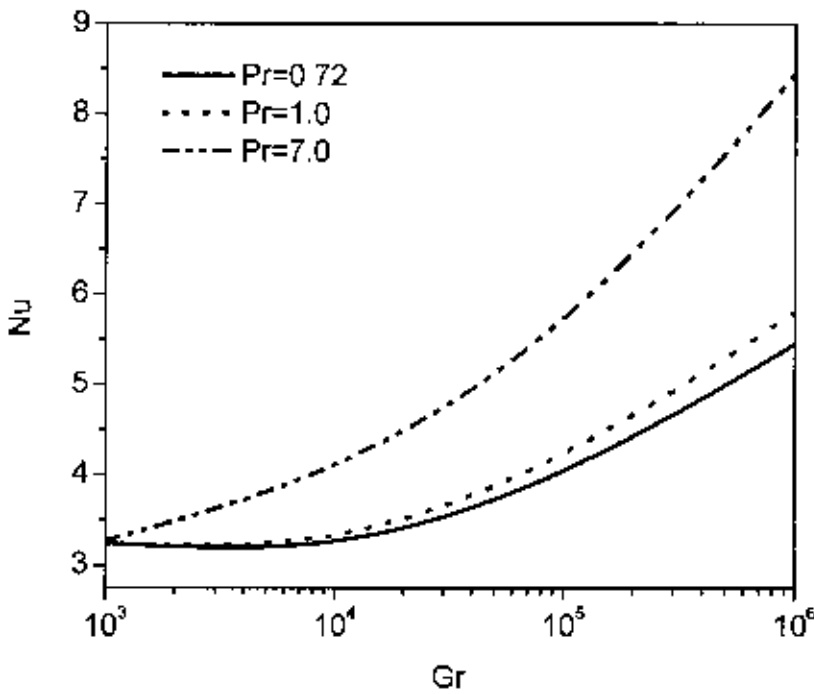while $Pr = 7.0$, $dr = 0.2$.

Fig.4.19: Effect of Prandtl number on average Nusselt number and Grashof number
while $Pr = 0.72$, 1.0 and 7.0, angle 0° and $dr = 0.2$
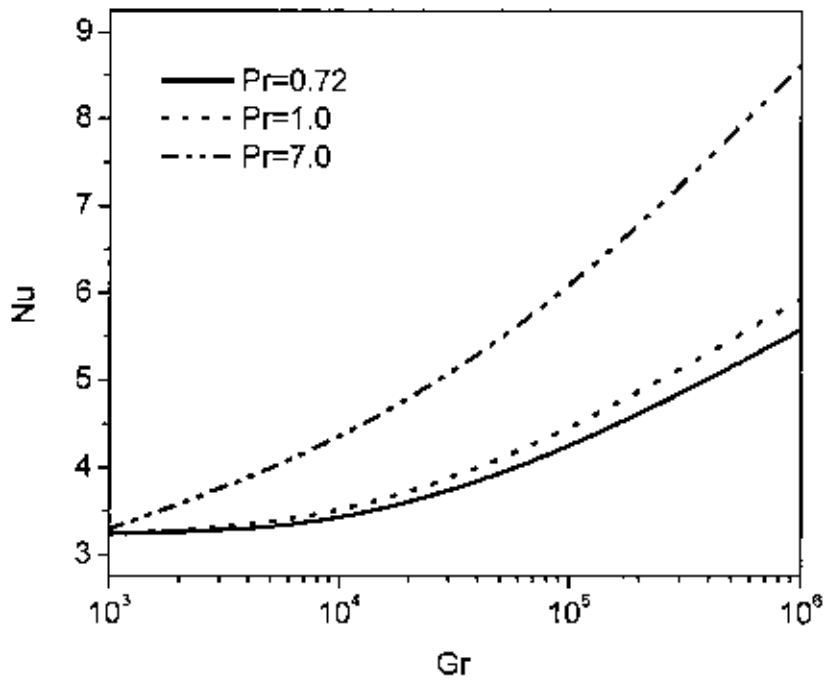
Fig.4.20: Effect of Prandtl number on average Nusselt number and Grashof number while $Pr = 0.72$, 1.0 and 7.0, angle 15° and $dr = 0.2$.

Fig.4.21: Effect of Prandtl number on average Nusselt number and Grashof number while $Pr = 0.72$, 1.0 and 7.0, angle 30° and $dr = 0.2$.
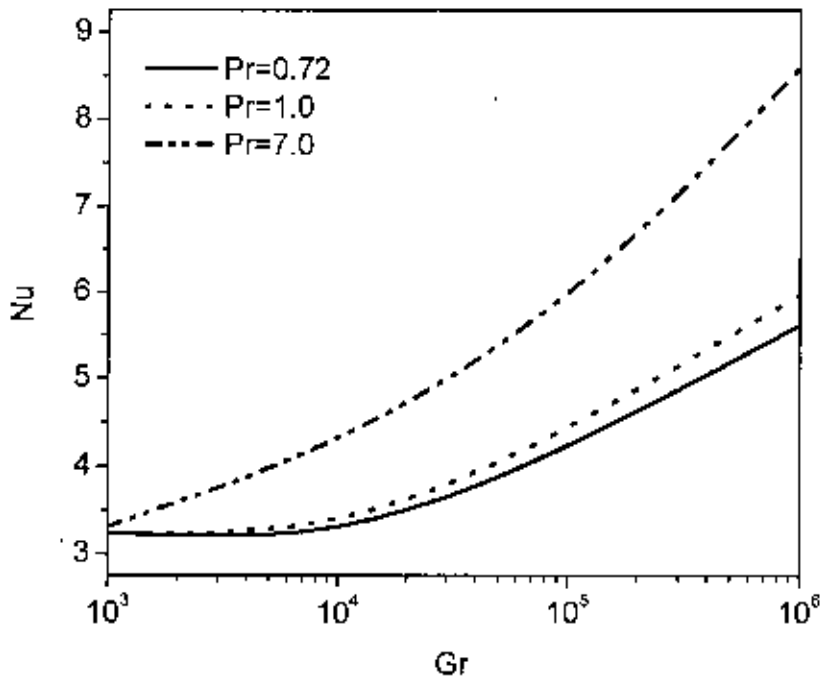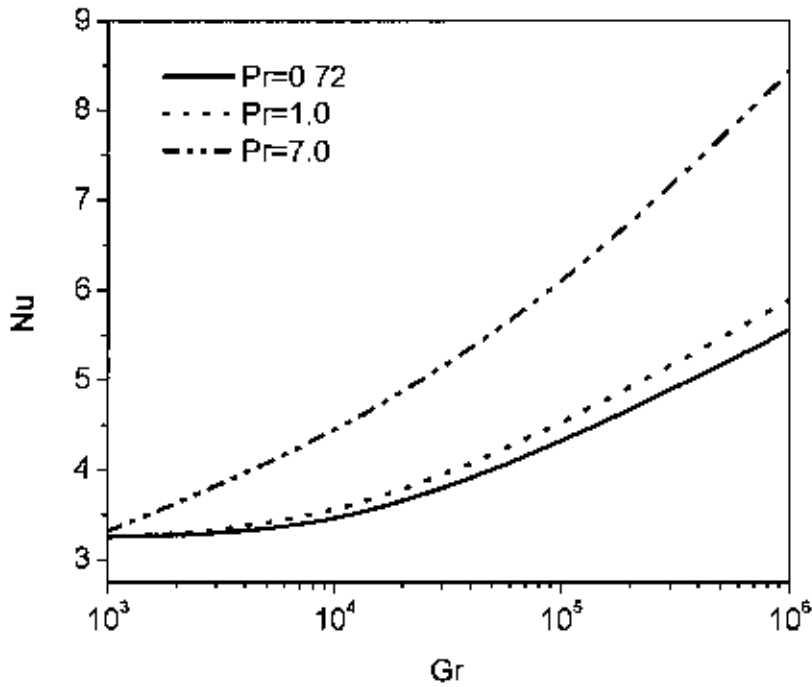
56

Fig.4.22: Effect of Prandtl number on average Nusselt number and Grashof number
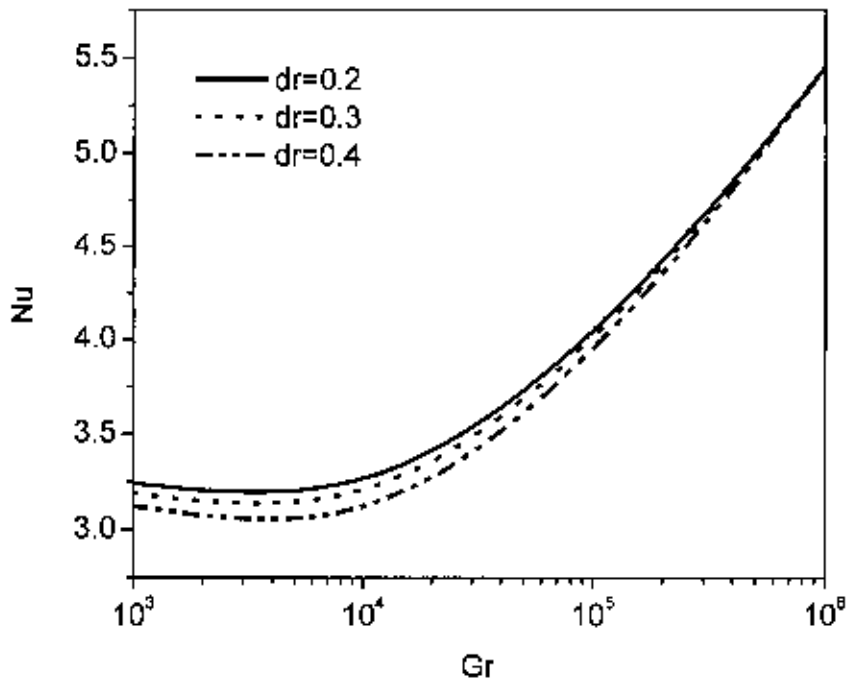while Pr = 0.72, 1.0 and 7.0, angle $45°$ and dr = 0.2.

Fig.4.23: Effect of diameter ratio on average Nusselt number and Grashof number
while Pr = 0.72, 1.0 and 7.0, angle $0°$.

REFERENCES

Arnold, J. N., Catton, I., and Edwards, D. K., "Experimental Investigation of Natural Convection in Inclined Rectangular Regions of Differing Aspect Ratios," Journal of Heat Transfer, Vol. 98, pp.67-71, 1976.

Bilgen, E., and Oztop, H., "Natural convection heat transfer in partially open inclined square cavities", Int. J. of Heat and Mass Transfer, Vol. 48, pp. 1470-1479, 2005. .

Chan, Y. L. and Tien, C. L.. "A Numerical study of two-dimensional laminar natural convection in a shallow open cavity", Int. J. Heat Mass Transfer, Vol. 28, pp. 603-612,1985.

Chan, Y. L. and Tien, C. L., "A Numerical study of two-dimensional natural convection in square open cavities", Numerical Heat Transfer, Vol. 8, pp. 65-80, 1985.

Chen, C. J. and Talaie, V., "Finite Analytic Numerical Solutions of Laminar Natural Convection in Two-Dimensional Inclined Rectangular.Enclosures," ASME paper 85-HT-10, 1985.

Cook, R. D., Malkus, D. S., and Plesha, M. E., "Concepts and applications of finite element analysis", Third Ed., John Wiley & Sons, New York, 1989.

De, A.K. and Dalal, A.,"A numerical study of natural convection around a square, horizontal, heated cylinder placed in an enclosure", Int. J. of Heat and Mass Transfer, Vol. 49, pp. 4608-4623, 2006.

Dechaumphai, P. Adaptive finite element technique for heat transfer problems, Energy, Heat & Mass transfer, Vol. 17, pp. 87-94, 1995.

Dechaumphai, P., Finite Element Method in Engineering, second Ed., Chulalongkorn University Press, Bangkok,1999.

Elsherbiny, S.M., Raithby, G. D., and Hollands, K. G. T., "Heat Transfer by Natural Convection across Vertical and Incline Air Layers", Transactions of the ASME, Vol. 104, pp. 96-102, 1982.

Frederick, R. L. "Natural convection in an inclined square enclosure with a partition attached to its cold wall", Int. J. Heat and Mass Transfer,Vol. 32, pp. 87–94, 1989.

Gallagher, R. H., Simon, B. R., Johnson, P. C. and Gross, J. F.. Finite elements in biomechanics, John Wiley & Sons, New York, 1982.

Goutam Saha, Sumon Saha and Md. Arif Hasan Mamun, "A Finite Element Method for Steady-State Natural Convection in a Square Tilt Open Cavity", ARPN Journal of Engineering and Applied Sciences, Vol. 2, No. 2, pp. 41-49, 2007.

Hamady, F. J., Lloyd, J. R., Yang, H. Q., and Yang, K. T., "Study of Local Natural convection Heat Transfer in an Inclined Enclosure," International Journal of Heat and Mass Transfer, Vol. 32, pp.1697-1708, 1989.

Hinojosa, J. F., Estrada, C. A., Cabanillas, R. E., and Alvarez, G., "Nusselt number for the natural convection and surface thermal radiation in a square tilted open cavity", Int. Com. In Heat and Mass Transfer, Vol. 32, pp. 1184-1192, 2005.

Jini, J., The finite element method in electromagnetics. John Wiley & Sons, New York, 1993.

Kangni, A., Ben, R. and Bilgen, E. "Natural convection and conduction in enclosure with multiplevertical partitions", Int. J. Heat and Mass Transfer,Vol. 34, pp. 2819–2825, 1991.

Kuhn, D. and Oosthuizen, P. H., "Unsteady natural convection in a partially heated rectangular cavity", ASME Journal of Heat Transfer, Vol. 109, pp. 789–801, 1987.

Kuyper, R.A., Van Der Meer, Th. H., Hoogendoorn, C. J., and Henkes, R. A. W. M., "Numerical Study of Laminar and Turbulent Natural Convection in an Inclined Square Cavity," International Journal of Heat and Mass Transfer, Vol. 36, No. 11, pp. 2899-2911, 1992.

Lakhal, E. K., Hasnaoui, M.and Vasseur, P., "Numerical study of transient natural convection in a cavity heated periodically with different types of excitations", International Journal of Heat and Mass Transfer, Vol. 42, No. 21, pp. 3927–3941, 1999.

Le Quere, P., Humphery, J. A., and Sherman, F.S. "Numerical calculation of thermally driven two-dimensional unsteady laminar flow in cavities of rectangular cross section", Numerical Heat Transfer, Vol. 4, pp. 249-283,1981.

Lewis, R.W., Morgan, K.. Thomas, H. R. and Seetharamu, K. N., The Finite element method in heat transfer analysis, John Wiley & Sons, New York, 1996.

Linthorst, S.J.M., Schinkel. W. M. M., and Hoogendorn, C. J.. "Flow Structure with Natural convection in Inclined Air-filled Enclosures," Journal of Heat Transfer. Vol. 103, pp.535-539, 1981.

Mohamad, A., "Natural convection in open cavities and slots", Numerical Heat Transfer, Vol. 27, pp. 705-716, 1995.

Ozoe, H., Sayama, H., and Churchill. S. W., "Natural Circulation in an Inclined Rectangular channel at Various Aspect Ratios and Angles—Experimental Measurements," International Journal of Heat and Mass Transfer, Vol.18, pp.1425-1420, 1975.

Ozoe, H., Sayama, H.. and Churchill, S. W., "Natural Convection in an Inclined Square Channel," International Journal of Heat and Mass Transfer, Vol. 17. pp.401-406,1974.

Patankar, S. V.. Numerical Heat Transfer and Fluid Flow, Hemisphere, Washington, DC; McGraw-Hill, New York, 1980.

Penot, F., "Numerical calculation of two-dimensional natural convection in isothermal open cavities", Numerical Heat Transfer, Vol. 5, pp. 421-437, 1982.

Peraire, J., Vahidati, M., Morgan, K., and Zienkiewicz, O. C. Adaptive remeshing for compressible flow computation, Journal of Computational Physics, Vol.72, pp. 449-466, 1987.

Polat, O. and Bilgen, E. "Laminar natural convection in inclined open shallow cavities", Int. J. Therm Sci, Vol. 41, pp. 360-368, 2002.

Showole, R.A. and Tarasuk, J.D., "Experimental and numerical studies of natural convection with flow separation in upward-facing inclined open cavities",Journal of Heat Transfer, Vol. 115, pp. 592-605, 1993.

Soong, C. Y., Tzeng, P. Y., Chiang, D. C., and Sheu, T. S., "Numerical Study on Mode-transition on Natural Convection in Differentially Heated Inclined Enclosures", International Journal of Heat and Mass Transfer, Vol. 39, No. 14, pp. 2869-2882, 1996.

Tasnim, S. T. and Collins, M.R. "Numerical analysis of heat transfer in a square cavity with a baffle on the hot wall", Int. Com. Heat and Mass Transfer, Vol. 31, pp. 639–650, 2004.

Zhao, Y., "Investigation of Heat Transfer Performance in Fenestration System Based on Finite Element Methods," Ph.D. Thesis, Department of Mechanical and Industrial Engineering, University of Massachusetts Amherst, 1997.

Zhong, Z.Y., Yang, K. T., and Lloyd, J. R., "Variable-property Natural convection in tilted Enclosures with Thermal Radiation", Numerical Methods in Heat Transfer, Vol. III, pp. 195-214, 1985.

Zienkiewicz, O. C. and Taylor, R. L. The finite element method, Fourth Ed., McGraw-Hill. 1991.